# Commensalistic Cultures with Kinetic Feedback—Static and Dynamic Behavior

**Satish J. Parulekar and Parag A. Ingle**
Dept. of Chemical and Environmental Engineering, Illinois Institute of Technology, Chicago, IL 60616

*DOI 10.1002/aic.10898*
*Published online June 27, 2006 in Wiley InterScience (www.interscience.wiley.com).*

*Steady state and dynamic behavior of continuous mixed cultures of two cell species with commensalistic interaction and kinetic feedback is investigated. The generation of the substrate required for growth of the host cell species from a primary resource is catalyzed by extracellular enzymes produced by the cell species, providing thereby, a kinetic feedback. The steady states are divided into three types. For the form of kinetics considered, the reactor can operate at up to seven steady states, including up to four steady states in which the cell species coexist. Conditions for admissibility and stability of different steady states are derived analytically. Admissibility of cyclic states is investigated. The specific example considered pertains to anaerobic digestion of complex insoluble organics by acid generating and methane generating bacteria. For a specific kinetic parameter set, the operating parameter space is divided into multiple regions based on admissibility of various steady states and dynamic characteristics. Startup policies to reach desired steady states are discussed.* © 2006 American Institute of Chemical Engineers *AIChE J,* 52: 2949–2963, 2006
*Keywords: biochemical engineering, bioprocess engineering, environmental engineering, fermentation, reactor analysis*

## Introduction

Microbial populations comprising of two or more different organisms and inhabiting a common environment are known to interact in a number of different ways.[1] The major interactions observed in a mixed culture of two organisms are competition, mutualism, commensalism, neutralism, amensalism, predation, and parasitism.[2–4] The dynamics of mixed cultures are important considerations in commercial fermentations involving wild-type and recombinant cell species, biological waste treatment, and ecological systems. Mixed cultures have been used extensively in manufacturing of food products, such as bread, cheese, yogurt, and pickles; fermentations of wines, beer, and whisky; pharmaceutical processes, such as transformation of steroids and manufacture of antibiotics and vitamins; biological waste treatment; and biological leaching processes.[5,6]

Correspondence concerning this article should be addressed to S.J. Parulekar at parulekar@iit.edu



Commensalism is an interaction in which one cell population (organism) is positively affected by the presence of the other, while the second population is not affected substantially by the presence of the first population.[2–4] Various mechanisms may result in a commensal interaction. Two of the most common mechanisms are:[4] (1) one population, the host population, generates a nutrient or a growth factor required for growth of the other population, the commensal population, and (2) one population generates a growth-inhibitory extracellular product, which is metabolized by the second population, but is not a required nutrient for the population. This work is concerned with the first mechanism.

While commensalistic cultures are frequently encountered in many ecosystems, they also have important applications in biological production processes and biological waste treatment processes (see[2–6] for citations on experimental and theoretical studies). The theoretical studies on commensalistic cultures have focused on CSTR operation, and have dealt with steady-state characteristics (multiplicity and local stability)[5,7–10] and dynamic behavior, including admissibility and stability of cyclic states.[5,10]

The specific example of commensalistic system considered in this study pertains to anaerobic digestion of complex insoluble organics. Anaerobic wastewater purification processes have been increasingly used in the recent years. Anaerobic digestion is a biological process in which organic matter is transformed by a community of microorganisms into biogas (primarily methane and carbon dioxide) in the absence of oxygen.[11–13] This process appears to be a promising method to solve some energy and ecological problems in agriculture and industry. Advantages this process has over the other common waste treatment process, the aerobic activated sludge process, include (1) much lower energy requirement; (2) generation of less sludge, curtailing thereby, the cost of energy-intensive post-treatment and disposal; and (3) generation of biogas, which can be used as an energy source.[14,15] In the past few years, a number of experimental studies aimed at improving the performance of anaerobic digestion,[16–18] and kinetic models for the process[11,19–23] have been reported. The process involves a consortium of acid generating bacteria (host population) and methane generating bacteria (commensal population). The initiation of this process requires hydrolysis of complex insoluble organics by extracellular enzymes synthesized by the host population to produce simple soluble organics, which can be utilized by the host population.

In this work, steady state and dynamic behavior of continuous mixed cultures of two cell species with commensalistic interaction and kinetic feedback is analyzed and investigated. The kinetic feedback adds to the complexity of the culture operation. Anaerobic digestion is considered as the example process. After presenting the problem formulation, classification of steady states and information on conditions for admissibility of and the maximum number of each steady state type are provided. This is followed by a summary of local stability analysis of various steady states, with details of the analysis, including derivation of criteria for stability and limit point and Hopf bifurcations, being relegated to the Appendix. For fruitful operation of the reaction process, retention of both cell species in the culture is essential. Exact criteria for admissibility of various steady states for which coexistence is possible are derived next, and for a specific kinetic parameter set, the operating parameter space is divided into multiple regions depending on the admissibility of various steady states. Classification of dynamic behavior of the mixed culture is provided next, suggesting startup policies to reach desired steady states. This is followed by numerical results, which illustrate bifurcation patterns of the coexistence steady states, and emergence and disappearance of these as the operating parameters are varied.

## Problem Formulation

The anaerobic degradation of organic matter is a complicated biological process. The conversion of organic matter consists of several independent, consecutive, and parallel reactions in which a close-knit community of bacteria cooperate to form a stable, self-regulating fermentation that transforms organic matter into a mixture of methane and carbon dioxide. These processes occur in six main stages, each carried out by one group of bacteria: hydrolysis of biopolymers into monomers (amino acids, sugars, and fatty acids), fermentation of amino acids and sugars, anaerobic oxidation of long-chain fatty acids and alcohols, anaerobic oxidation of volatile fatty acids, conversion of acetate to methane, and conversion of hydrogen to methane.[24] Many mechanistic models of varying complexity have been proposed for description of kinetics of anaerobic digestion.[24–27] While these models include multiple bacterial groups and many lumped chemical species and consider many reaction steps, a large number of kinetic parameters in these cannot be determined from the limited amount of experimental data available and must be assigned *a priori.* This places a serious limitation on predictive ability of these kinetic models. As an alternative, simpler kinetic models have been developed, based on the complex mechanistic models to predict the dynamic behavior of anaerobic digesters. The six groups of bacteria are divided into two major groups: acid producing microorganisms and methane producing microorganisms.[19,22,24,26] The simpler kinetic models also have a large number of parameters, which can be determined from the available experimental data base.[22] A large body of information on the ranges of the kinetic parameters in these models is available.[22]

A detailed analysis of static and dynamic behavior of anaerobic digestion in a continuous flow stirred-tank reactor (CSTR) is presented in this manuscript. A modified version of Hill and Barth's model,[19,22] which provides a concise three-stage representation of this complex process incorporating mixed consortia of microorganisms, is adopted here. This process involves two types of bacteria, namely acid producing bacteria or *acidogens* ($X$) and methane producing bacteria or *methanogens* ($Y$), and can be concisely represented as

$$A \xrightarrow{E} B \xrightarrow{X} C \xrightarrow{Y} P \tag{1}$$

The reactor feed is comprised of complex insoluble organics (polysaccharides, lipids, proteins, and nucleic acids), $A$, which are hydrolyzed by extracellular enzymes, $E$, to simple soluble organics (sugars, fatty acids, amino acids, purines, pyrimidines, cellobiose, and glycerol), $B$. The extracellular enzymes are synthesized and secreted by the acidogens. The acidogens utilize $B$ for their growth and generate volatile acids $C$, such as acetic, formic, and propionic acids. The methanogens utilize $C$ for their growth and generate, among other products, biogas, $P$, which is comprised largely of methane and carbon dioxide. Commensalistic cultures are described by the second and third steps in Eq. 1, with $B$ being supplied in the reactor feed in continuous culture operation.

The first step in Eq. 1 involves a feedback effect of $X$ ($E$ synthesized by $X$), adding to complexity of the process. Such kinetic feedback also occurs in other cell cultures, two notable examples being conversion of cellulose and starch by suitable cell species to target metabolites. Utilization of these substrates requires synthesis of extracellular enzymes, cellulases in the case of cellulose and amylases in the case of starch, by living cells. The extracellular enzymes catalyze the hydrolysis of cellulose and starch to glucose, which can then be metabolized by living cells to allow for their growth and production of target metabolites.

Among the species involved in the representation in Eq. 1, the feed to the CSTR contains only $A$. The conservation equations for the species in Eq. 1 influencing the kinetics are then stated as

$$\frac{dA}{dt} = f_1, \qquad f_1 = D(A_0 - A) - r_1 \tag{2}$$

$$\frac{dX}{dt} = f_2, \qquad f_2 = -DX + (\mu_1 - k_1)X \tag{3}$$

$$\frac{dB}{dt} = f_3, \qquad f_3 = -DB + r_1 - \beta\mu_1 X \tag{4}$$

$$\frac{dY}{dt} = f_4, \qquad f_4 = -DY + (\mu_2 - k_2)Y \tag{5}$$

$$\frac{dC}{dt} = f_5, \qquad f_5 = -DC + \gamma\mu_1 X - \delta\mu_2 Y \tag{6}$$

with the biogas production rate $Q$, being expressed as

$$Q = \varepsilon\mu_2 Y \tag{7}$$

Due to the very restrictive online information, the control of the process is often reduced to regulation of the biogas production rate ($Q$). For this reason, $Q$ is considered to be an important indicator of the performance of the mixed culture.[12]

The conservation equations, Eqs. 2–6, are based on steady state operation as concerns total mass in the reactor, with densities of the feed and effluent streams being equal and time-invariant. The operating volume of the reactor is, therefore, considered to be time-invariant. It is also assumed that the volume fraction of the biotic phase in the culture is not significant. Concentrations of all species can, therefore, be based on the culture volume.

In Eqs. 2–7, the parameters $k_1$, $k_2$, $\beta$, $\gamma$, $\delta$, and $\varepsilon$ are considered to be independent of the culture composition. The expressions for $r_1$, $\mu_1$ and $\mu_2$ are[22]

$$r_1 = \alpha AX, \qquad \mu_1 = \frac{\mu_{10}B}{(K_1 + B)},$$

$$\mu_2 = \frac{\mu_{20}C}{(K_2 + C)\left(1 + \frac{C}{K_I}\right)} \tag{8}$$

**Table 1. Values of Kinetic Parameters in Eqs. 2–8**

| Parameter | Value | Units |
|---|---|---|
| $k_1$ | $4.63 \times 10^{-8}$ | $s^{-1}$ |
| $k_2$ | $4.63 \times 10^{-8}$ | $s^{-1}$ |
| $K_1$ | 0.16 | $kg/m^3$ |
| $K_2$ | $8.2 \times 10^{-4}$ | $kg/m^3$ |
| $K_I$ | 0.04185 | $kg/m^3$ |
| $\alpha$ | $5.787 \times 10^{-3}$ | $m^3/\{kg\ X \cdot s\}$ |
| $\beta$ | 37.8787 | kg B/kg $X$ |
| $\gamma$ | 2.45 | kg C/kg $X$ |
| $\delta$ | 41.3223 | kg C/kg $Y$ |
| $\varepsilon$ | 74.54 | $\{m^3\ P\}\{m^3$ culture$\}$/kg $Y$ |
| $\mu_{10}$ | $4.63 \times 10^{-6}$ | $s^{-1}$ |
| $\mu_{20}$ | $4.63 \times 10^{-6}$ | $s^{-1}$ |

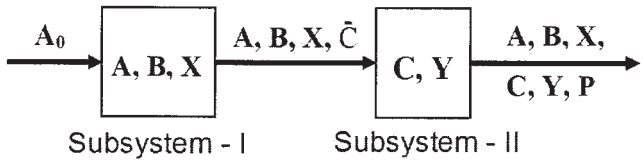


**Figure 1. Compartmentalization of the reaction system**

with $\alpha$, $\mu_{j0}$, $K_j$ ($j = 1, 2$) and $K_I$ being independent of the culture composition. The kinetic model in Eqs. 2–8 contains 12 parameters. The model and its special cases have been used in several prior studies, and a large body of information on the ranges of the kinetic parameters is available.[22] The robustness of the kinetic model, which captures the key regulatory effects in anaerobic digestion, has been tested in some of the prior studies. This was the motivation for the use of the model in this study.

The rate of hydrolysis of $A$ by $E$ is related to the concentrations of $A$ and $X$ since $E$ is synthesized by $X$, and, thus, has second-order kinetics. The rate of generation of the growth-limiting substrate for $X$, $B$, from its precursor, $A$, is, thus, dictated by $X$, providing a kinetic feedback. The rates of utilization of $B$ and $C$ by $X$ and $Y$, respectively, are linearly related to the respective growth rates. The base set of parameters in Eqs. 2–8 is provided in Table 1. For the expressions in Eq. 8, the maximum specific growth rates of $X$ and $Y$, $\mu_{1m}$ and $\mu_{2m}$, respectively, can be deduced to be

$$\mu_{1m} = \mu_{10} \text{ as } B \to \infty \text{ and } \mu_{2m} = \frac{\mu_{20}}{\left(1 + \sqrt{\frac{K_2}{K_I}}\right)^2} \text{ at}$$

$$C = C_m = \sqrt{K_2 K_I} \tag{9}$$

Since the kinetics of generation/utilization of $A$, $B$, and $X$ are not affected by concentrations of $C$ and $Y$ (no feedback effect), the reactor model can be represented as a two-compartment model (Figure 1). This compartmentalization simplifies considerably the analysis of steady-state types and stability characteristics of these and classification of dynamic behavior.

## Steady-State Analysis

### *Steady state types*

The steady-state solutions are characterized by time-invariance of $A$, $B$, $C$, $X$ and $Y$ and are, therefore, provided by $f_j = 0$, $j = 1 - 5$. Since the interaction observed in the mixed culture here is commensalism, with $Y$ being dependent on $X$ through the substrate ($C$) for the former, three types of steady states are admissible. These are (a) total washout steady state ($TW$): $X = 0$, $Y = 0$ (neither organism retained in the reactor), (b) partial washout steady state ($PW$): $X > 0$, $Y = 0$ (only $X$ retained in the reactor), and (c) coexistence steady state ($CO$): $X > 0$, $Y > 0$ (both $X$ and $Y$ retained in the reactor). The steady state where $X = 0$ and $Y > 0$, requires ($DC + \delta\mu_2 Y$) to be zero (Eq. 6), which is not possible since $C$ is non-negative.

Since species $X$ and $Y$ play a vital role in the process, it is prudent to look at solutions of mass balances for these, $f_2 = 0$ and $f_4 = 0$ (Eqs. 3 and 5), viz., $X = 0$ and/or

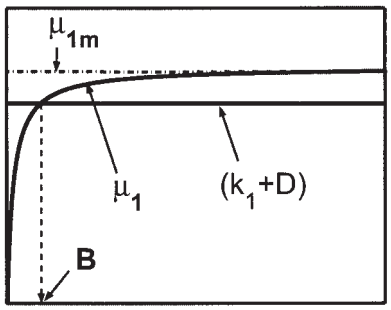


(a)

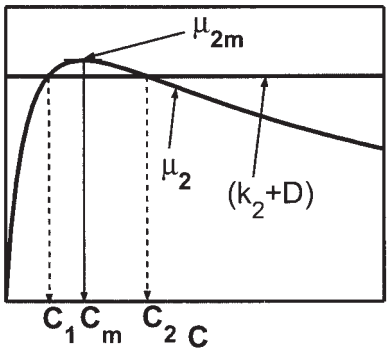


(b)

**Figure 2. Representation of (a) Eq. 10 and (b) Eq. 11.**

The curves indicate profiles of (a) $\mu_1$ and (b) $\mu_2$, and the horizontal lines indicate (a) $(k_1 + D)$, and (b) $(k_2 + D)$.

$$\mu_1 = (k_1 + D) < \mu_{1m} \quad \text{if} \quad X > 0 \tag{10}$$

and $Y = 0$ and/or

$$\mu_2 = (k_2 + D) \leq \mu_{2m} \quad \text{if} \quad Y > 0 \tag{11}$$

Equation 10 must be satisfied for partial washout and coexistence steady states; additionally, for a coexistence steady state, Eq. 11 must also be satisfied.

Substitution of $\mu_1$ in Eq. 8 into Eq. 10 leads to $B$ at steady state as

$$B = \frac{K_1(k_1 + D)}{\mu_{10} - (k_1 + D)} \tag{12}$$

It is evident from Eq. 12 and Figure 2a that for fixed $D$, only one steady-state value of $B$ is possible with $X$ retained in the culture.

Similarly, substituting $\mu_2$ in Eq. 8 into Eq. 11 leads to the following expressions for $C$, $C = C_1$, $C_2$, with $C_1$ and $C_2$ being

$$C_1 = \frac{K_I}{2}[\xi - \nu], \qquad C_2 = \frac{K_I}{2}[\xi + \nu],$$

$$\xi = \left[\frac{\mu_{20}}{(k_2 + D)} - \left(1 + \frac{K_2}{K_I}\right)\right], \qquad \nu = \sqrt{\xi^2 - 4\,\frac{K_2}{K_I}} \tag{13}$$

For fixed $D$, therefore, up to two steady-state values of $C$ are possible with $Y$ retained in the culture (Figure 2b).

### *Number of each steady state type*

For a total washout steady state ($X = 0$, $Y = 0$), it follows from Eqs. 2, 4, and 6 that $A = A_0$ and $B = C = 0$. This steady state is, therefore, unique. For any steady state, one obtains from Eqs. 2, 4, and 8 the following

$$A = \frac{DA_0}{(D + \alpha X)}, \qquad X = \frac{DB}{(\alpha A - \beta\mu_1)} \tag{14}$$

Addition of Eqs. 2 and 4 leads to

$$(A_0 - A - B) = \beta\,\frac{(k_1 + D)}{D}\,X \tag{15}$$

Substitution of expression for $A$ in Eq. 14 into Eq. 15 leads to a quadratic equation for $X$ in terms of the kinetic parameters and the two operating parameters, $D$ and $A_0$, as

$$\alpha\beta(k_1 + D)X^2 - \phi X + D^2B = 0,$$
$$\phi = D[\alpha(A_0 - B) - \beta(k_1 + D)] \tag{16}$$

Real valued positive solutions ($X > 0$) are not possible when $\phi \leq 0$. When $\phi > 0$, the expressions for $X$ at steady state, $X_1$ and $X_2$, are

$$X_1 = \frac{\phi - \sqrt{\Delta}}{2\alpha\beta(k_1 + D)}, \qquad X_2 = \frac{\phi + \sqrt{\Delta}}{2\alpha\beta(k_1 + D)},$$
$$\Delta = [\phi^2 - 4\alpha\beta(k_1 + D)D^2B] \tag{17}$$

The solutions in Eq. 17 are real-valued if, and only if $\Delta \geq 0$. After some algebraic manipulation, this condition can be reduced to ($B$ related to $D$ as per Eq. 12)

$$A_0 \geq \psi(D), \qquad \psi(D) = B + \frac{1}{\alpha}[\beta(k_1 + D) + \sqrt{4\alpha\beta(k_1 + D)B}] \tag{18}$$

It follows from the definition of $\Delta$ in Eq. 17 that when $\Delta \geq 0$, $\sqrt{\Delta} \leq \phi$, and $X_1$ and $X_2$ are positive. Further, $X_1 < X_2$ when $\Delta > 0$ or $A_0 > \psi(D)$ and $X_1 = X_2$ when $\Delta = 0$ or $A_0 = \psi(D)$. From Eq. 14, it is evident that for fixed $D$ and $A_0$, there is one-to-one correspondence between $A$ and $X$, and the maximum number of solutions of Eqs. 2–4, such that $X > 0$, therefore, is two. In summary, the number of solutions of Eqs. 2–4 with positive $X$ is (1) zero if $A_0 < \psi(D)$, (2) one if $A_0 = \psi(D)$ $(X_1 = X_2)$, and (3) two if $A_0 > \psi(D)$ $(X_2 > X_1)$. The profile of $\psi$ for the parameters listed in Table 1 is shown in Figure 3.

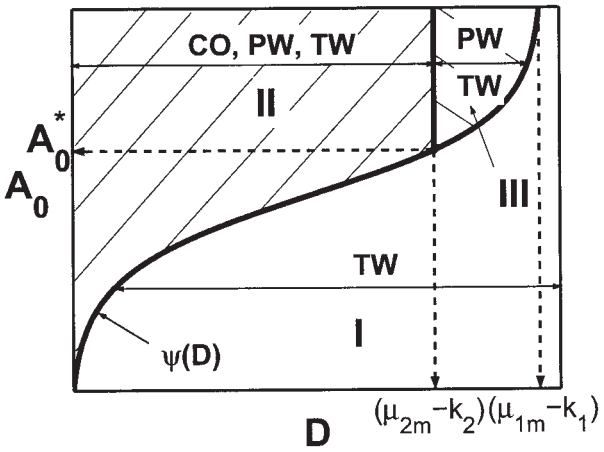


**Figure 3. Division of ($D$, $A_0$) space in terms of retention of $X$ and $Y$ at steady state.**

The curve represents $\psi(D)$. Retention of $X$ occurs for $A_0 \geq \psi(D)$, $0 < D < (\mu_{1m} - k_1)$, and that of $Y$ occurs for $A_0 \geq \psi(D)$, $0 < D \leq (\mu_{2m} - k_2)$.

For a steady-state operation with $X > 0$, Eq. 6 can be rearranged as

$$C = \left[\bar{C} - \frac{\delta\mu_2 Y}{D}\right], \qquad \bar{C} = \frac{\gamma(k_1 + D)X}{D} \tag{19}$$

For a particular $D$, let $\bar{C}_1 = \bar{C}(X_1)$ and $\bar{C}_2 = \bar{C}(X_2)$. Since $X_1 \leq X_2$, it follows that $\bar{C}_1 \leq \bar{C}_2$. It also follows that (1) $C = \bar{C}$ for a partial washout steady state ($PW$, $Y = 0$) and (2) $C < \bar{C}$ for a coexistence steady state ($CO$, $Y > 0$). For a coexistence steady state, $C = C_1, C_2$, with $C_1$ and $C_2$ being defined in Eq. 13. For a particular $X$, the number of coexistence steady states is (1) zero if $\bar{C} \leq C_1$, (2) one if $C_1 < \bar{C} \leq C_2$, or (3) two if $\bar{C} > C_2$ (Figure 2b). In conjunction with the observations on the number of solutions of mass balances for $A$, $B$ and $X$ (Eqs. 2–4), it can be deduced that the maximum number of coexistence steady states is four. The notation for the partial washout and coexistence steady states is provided in Table 2 and will be used where needed in the remainder of this article.

Coexistence steady states are possible only when Eqs. 10 and 11 are satisfied, that is, when $D \leq \min[(\mu_{1m} - k_1), (\mu_{2m} - k_2)]$. For the parameters listed in Table 1, $(\mu_{1m} - k_1) > (\mu_{2m} - k_2)$, and coexistence steady states are, therefore, admissible for $0 < D \leq (\mu_{2m} - k_2)$ provided $A_0 \geq \psi(D)$ (Eq. 18). For $A_0 = \psi(D)$, $X_1 = X_2$ and, therefore, $\bar{C}_1 = \bar{C}_2$, and only $CO1$ and $CO3$ are possible (Table 2). When $D = (\mu_{2m} - k_2)$, we have $C_1 = C_2 = C_m$, and this permits the possibility of existence of only $CO3$ and $CO4$ for $A_0 > \psi(D)$, and only $CO3$ for $A_0 = \psi(D)$.

Partial washout states are possible only when $D < (\mu_{1m} - k_1)$ (Eq. 10) and $A_0 \geq \psi(D)$. The steady states of this type admissible then are (1) $PW1$ if $A_0 = \psi(D)$ ($X_1 = X_2$), and (2) $PW1$ and $PW2$ if $A_0 > \psi(D)$ ($X_2 > X_1$).

## Local Stability of Steady States

A summary of the stability analysis of various steady states is provided here, with the details on derivation of criteria for stability and bifurcation being provided in the Appendix. While the total washout steady state ($TW$) is locally stable for $D > 0$, among the six steady states, where $X$ is retained (Table 2), only two, $PW2$ and $CO2$, *may be* locally stable. Only these steady states may, therefore, undergo static and Hopf bifurcations. Both steady states correspond to higher value of $X$, $X_2$, and hence higher $\bar{C}$, $\bar{C}_2$, which are the performance indicators for subsystem I and sources for subsystem II. Among the four coexistence steady states, the two exhibiting substrate inhibition for growth of commensal population $Y$, $CO3$ and $CO4$, are unstable and so is the steady state $CO1$, corresponding to inferior performance of subsystem $I$ ($X = X_1$). It will be seen later that the only possibly stable coexistence steady state $CO2$, also is the most efficient one as concerns the rate of generation of the desired product, $Q$. These results are indicative of the built-in regulation that the unstructured kinetic representation considered here has.

## Exact Criteria for Admissibility of Coexistence Steady States

One can restate Eq. 19 to obtain $Y$ as

$$Y = (aX - bC) = b(\bar{C} - C), \qquad a = \frac{\gamma(k_1 + D)}{\delta(k_2 + D)}, \qquad b = \frac{D}{\delta(k_2 + D)} \tag{20}$$

Physical realizability of a coexistence steady state requires that $Y$ be positive. Using the above, and the information in Table 2, we obtain the following

$$CO1\text{: } Y_1 = b(\bar{C}_1 - C_1), \qquad CO2\text{: } Y_2 = b(\bar{C}_2 - C_1), \qquad CO3\text{: } Y_3 = b(\bar{C}_1 - C_2)$$

$$CO4\text{: } Y_4 = b(\bar{C}_2 - C_2), \qquad \bar{C}_1 = \frac{\gamma(k_1 + D)X_1}{D}, \qquad \bar{C}_2 = \frac{\gamma(k_1 + D)X_2}{D} \tag{21}$$

Since $C_2 \geq C_1$ and $X_2 \geq X_1$ (and, therefore, $\bar{C}_2 \geq \bar{C}_1$), it follows that

$$Y_2 \geq Y_1 \geq Y_3 \quad \text{and} \quad Y_2 \geq Y_4 \geq Y_3 \tag{22}$$

**Table 2. Possible Partial Washout and Coexistence Steady States ($\bar{C}$ defined in Eq. 19)**

| Steady State | $X$ | $C$ | Stability | Steady State | $X$ | $C$ | Stability |
|---|---|---|---|---|---|---|---|
| $PW1$ | $X_1$ | $\bar{C}_1$ | Unstable | $PW2$ | $X_2$ | $\bar{C}_2$ | Stable/Unstable |
| $CO1$ | $X_1$ | $C_1$ | Unstable | $CO2$ | $X_2$ | $C_1$ | Stable/Unstable |
| $CO3$ | $X_1$ | $C_2$ | Unstable | $CO4$ | $X_2$ | $C_2$ | Unstable |

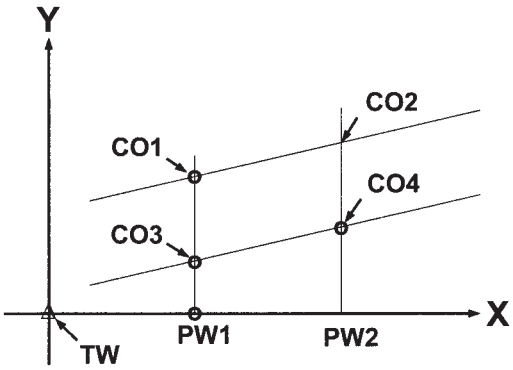


**Figure 4. Representations of the seven steady states in terms of their projections in the (*X*, *Y*) plane.**

Unstable steady states are indicated by '**o**' and the stable *TW* by 'Δ'

For particular $D$ and $A_0$, the specific rate of production of the end product, biogas, is proportional to $Y$ (Eqs. 7 and 11). Among the four coexistence steady states, $Q$ is, therefore, highest for $CO2$. It must be realized that among the four coexistence steady states, only one, $CO2$, *may be* locally stable (Table 2). The other three coexistence steady states, which lead to inferior $Y$ and $Q$, are unstable. These results are reflective of the regulatory effects in the unstructured kinetic representation considered here. From the expressions earlier, it is evident that for retention of $Y$ in a culture at steady state, it is *necessary* that $\bar{C}_2 > C_1$. From the relations in Eqs. 12, 13, 16, 17, and 19 it is evident that $C_1$ and $\bar{C}_2$ can be expressed explicitly in terms of the operating parameters $D$ and $A_0$.

The seven possible steady states can be conveniently represented by their projections in the $(X, Y)$ plane. In this plane, the steady states $CO1$ and $CO2$ lie on the line $Y = aX - bC_1$ and the steady states $CO3$ and $CO4$ lie on the line $Y = aX - bC_2$ (Figure 4). Depending on the mutual dispositions of $C_1$, $C_2$, $\bar{C}_1$, and $\bar{C}_2$, different scenarios with zero to four coexistence steady states arise. These are described in Table 3, with $D^* = (\mu_{2m} - k_2)$, and $A_0^* = \psi(D^*)$. One or more coexistence steady states are physically realizable in scenarios 3–12, 15–17, 20, and 23–25. Coexistence steady states are born from partial washout steady states in the following scenarios (numbers in parentheses): (2) $CO2$ from $PW2$, (4, 9, 14, 19) $CO1$ from $PW1$, (5, 8, 22) $CO4$ from $PW2$, and (11, 16, 24) $CO3$ from $PW1$. Retention of $X$ in the large ($t \to \infty$) implies retention of $Y$, provided it is present initially in the culture, for scenarios 3–6 and 8, since $PW2$ is unstable (Eq. A13). For scenarios 7 and 9–12, stability (instability) of $CO2$ implies stability (instability) of $PW2$ and vice versa (Eq. A13) and existence of cyclic states associated with $CO2$ implies existence of cyclic states associated with $PW2$ and vice versa (Eq. A19). Reactor operation at operating conditions that lead to scenarios 1, 2, 13, 14, 18, 19, 21, and 22 is not of interest since coexistence is not possible for any of these. Similarly, reactor operation at operating conditions that lead to scenarios 15–17, 20, and 23–25 is not of interest since stable coexistence is not possible for any of these. Stabilization of the unstable coexistence steady state(s) in these scenarios could be accomplished using a feedback controller. Such stabilization, however, is not of interest since the mixed culture operation in these scenarios will be suboptimal, as concerns $Y$ and $Q$, when compared to operation in scenarios 3–12. The numerical results to be presented later will reveal this.

Since $X_1 = X_2$ on the curve $A_0 = \psi(D)$, this curve represents the locus of limit points (collision of two steady states) for $PW1$ and $PW2$ (scenarios 13–17 in Table 3). It also represents the locus of limit points for the pairs (1) $CO1$ and $CO2$ and (2) $CO3$ and $CO4$, provided the steady states are physically realizable (Table 2 and scenarios 13–17 in Table 3).

From Figure 3, it is obvious that coexistence steady states may be admissible for $A_0 \geq \psi(D)$ in the interval $0 < D < D^*$ and for $A_0 \geq A_0^*$ when $D = D^*$. The portion of the vertical line $D = D^*$ ($C_1 = C_2$) in Figure 3 with $A_0 \geq A_0^*$ then represents the locus of limit points for the pairs (1) $CO1$ and $CO3$ and (2) $CO2$ and $CO4$, provided the steady states are physically realizable (scenarios 21–25 in Table 3). The maximum number of coexistence steady states on the curve $A_0 = \psi(D)$ with $0 < D < D^*$, and on the line $D = D^*$ with $A_0 > A_0^*$ is, therefore, two. At the point, $(D, A_0) = (D^*, A_0^*)$, there can be at the most one coexistence steady state as $C_1 = C_2$ and $\bar{C}_1 = \bar{C}_2$ (collision of two limit points, scenarios 18–20 in Table 3).

For $A_0 \geq \psi(D)$, it has been shown before that $B$, $X_1$ and $X_2$ are positive (Eqs. 12, 16 and 17) and it follows from Eq. 14 that $0 < A(X_i) < A_0$, $i = 1, 2$. For $0 < D \leq D^*$, $C_1$ and $C_2$ are positive (Figure 2b). Furthermore, the concentrations of $A$, $B$, $C$ and $X$ for all coexistence steady states are bounded. Therefore, the only reason a coexistence steady state may not be physically realizable is that $Y$ for that steady state provided in

**Table 3. Exact Criteria for Coexistence Steady States**

| No. | Conditions | $COj$, $j$ = 1–4 | $PW2$ fate[a] |
|---|---|---|---|
| 1 | $\bar{C}_1 < \bar{C}_2 < C_1 < C_2$ | None | — |
| 2 | $\bar{C}_1 < \bar{C}_2 = C_1 < C_2$ | None | U |
| 3 | $\bar{C}_1 < C_1 < \bar{C}_2 < C_2$ | 2 | U |
| 4 | $\bar{C}_1 = C_1 < \bar{C}_2 < C_2$ | 2 | U |
| 5 | $\bar{C}_1 < C_1 < \bar{C}_2 = C_2$ | 2 | U |
| 6 | $C_1 < \bar{C}_1 < \bar{C}_2 < C_2$ | 1, 2 | U |
| 7 | $\bar{C}_1 < C_1 < C_2 < \bar{C}_2$ | 2, 4 | —* |
| 8 | $C_1 < \bar{C}_1 < C_2 = \bar{C}_2$ | 1, 2 | U |
| 9 | $\bar{C}_1 = C_1 < C_2 < \bar{C}_2$ | 2, 4 | —* |
| 10 | $C_1 < \bar{C}_1 < C_2 < \bar{C}_2$ | 1, 2, 4 | —* |
| 11 | $C_1 < C_2 = \bar{C}_1 < \bar{C}_2$ | 1, 2, 4 | —* |
| 12 | $C_1 < C_2 < \bar{C}_1 < \bar{C}_2$ | 1, 2, 3, 4 | —* |
| 13 | $\bar{C}_1 = \bar{C}_2 < C_1 < C_2$ | None | U |
| 14 | $\bar{C}_1 = \bar{C}_2 = C_1 < C_2$ | None | U |
| 15 | $C_1 < \bar{C}_1 = \bar{C}_2 < C_2$ | 1 | U |
| 16 | $C_1 < \bar{C}_1 = \bar{C}_2 = C_2$ | 1 | U |
| 17 | $C_1 < C_2 < \bar{C}_1 = \bar{C}_2$ | 1, 3 | U |
| 18 | $\bar{C}_1 = \bar{C}_2 < C_1 = C_2$ | None | U |
| 19 | $\bar{C}_1 = \bar{C}_2 = C_1 = C_2$ | None | U |
| 20 | $C_1 = C_2 < \bar{C}_1 = \bar{C}_2$ | 1 | U |
| 21 | $\bar{C}_1 < \bar{C}_2 < C_1 = C_2$ | None | — |
| 22 | $\bar{C}_1 < \bar{C}_2 = C_1 = C_2$ | None | U |
| 23 | $\bar{C}_1 < C_1 = C_2 < \bar{C}_2$ | 4 | — |
| 24 | $\bar{C}_1 = C_1 = C_2 < \bar{C}_2$ | 4 | — |
| 25 | $C_1 = C_2 < \bar{C}_1 < \bar{C}_2$ | 3, 4 | — |

| Scenarios | Range of $D$ | Range of $A_0$ |
|---|---|---|
| 1–12 | $0 < D < D^*$ | $A_0 > \psi(D)$ |
| 13–17 | $0 < D < D^*$ | $A_0 = \psi(D)$ |
| 18–20 | $D = D^*$ | $A_0 = A_0^* = \psi(D^*)$ |
| 21–25 | $D = D^*$ | $A_0 > \psi(D^*)$ |

[a] [U - unstable, '-' - stable (unstable) if $b_1 > 0$ ($b_1 < 0$), '*' - fate same as that of $CO2$ (stable/unstable/Hopf bifurcation)]

Eq. 21 may be non-positive. For a particular set of operating conditions, if $Y = 0$ in Eq. 21 for a coexistence steady state, then that steady state is born from the appropriate partial washout steady state. Steady states $CO1$ and $CO3$ branch off from $PW1$ and $CO2$ and $CO4$ branch off from $PW2$. In the $(D, A_0)$ space, the number of physically realizable coexistence steady states will change as one crosses the curves $Y_k = 0$, $k = 1$–4.

It is evident from Eq. 20 that the change in the number of coexistence steady states can be investigated by examining if and when

$$\bar{C}_i = C_j \text{ or } X_i = \frac{DC_j}{\gamma(k_1 + D)}, \qquad i, j = 1, 2 \tag{23}$$

with $C_j$, $\bar{C}_i$, and $X_i$ being defined in Eqs. 13, 17, and 21. This can be deduced to be equivalent to investigating the roots of

$$g_i = h_j, \qquad h_j = \frac{2\alpha\beta DC_j}{\gamma}, \qquad i, j = 1, 2$$

$$g_1 = \phi - \sqrt{\phi^2 - \zeta}, \qquad g_2 = \phi + \sqrt{\phi^2 - \zeta},$$

$$\zeta = 4\alpha\beta(k_1 + D)D^2B \tag{24}$$

In the above, $g_1$ corresponds to $X_1$ and $\bar{C}_1$ ($CO1$, $CO3$), and $g_2$ corresponds to $X_2$ and $\bar{C}_2$ ($CO2$, $CO4$) (Eq. 17). Since $X_1$ and $X_2$ are positive for $A_0 \geq \psi(D)$, so are $g_1$ and $g_2$, with $g_2 = g_1$ for $A_0 = \psi(D)$ and $g_2 > g_1$ for $A_0 > \psi(D)$. Furthermore, $h_2 > h_1$ when $C_2 > C_1$ ($0 < D < D^*$), and $h_1 = h_2$ when $C_1 = C_2$ ($D = D^*$). It is convenient to investigate the roots of Eq. 24 for a particular $D$ since, with the exception of $\phi$, all other terms in Eq. 24 are independent of $A_0$. For fixed $D$, $\phi$ varies linearly with $A_0$ (Eq. 16) and, therefore, it is not difficult to deduce that

$$\frac{\partial g_1}{\partial A_0} = -\frac{\alpha D g_1}{\sqrt{\phi^2 - \zeta}}, \qquad \frac{\partial g_2}{\partial A_0} = \frac{\alpha D g_2}{\sqrt{\phi^2 - \zeta}} \tag{25}$$

Therefore, $g_1$ decreases and $g_2$ increases as $A_0$ is increased. Both $\partial g_1/\partial A_0$ and $\partial g_2/\partial A_0$ become unbounded as $A_0 \to \psi(D)$. For $A_0 = \psi(D)$, $g_2 = g_1 = \sqrt{\zeta}$ and $g_2 > \sqrt{\zeta} > g_1$ for $A_0 > \psi(D)$. Using this information, the dispositions of $g_1$, $g_2$, $h_1$ and $h_2$ are displayed in Figure 5. Let $A_{01}$ and $A_{02}$ denote $A_0$ corresponding to intersection of (1) $h_1$ and $g_1$ or $g_2$, and (2) $h_2$ and $g_1$ or $g_2$, respectively. For a coexistence steady state to be physically realizable, $g_i$ for the steady state must exceed $h_j$ for the same. The following conclusions can then be drawn regarding admissibility (physical realization) of coexistence steady states at a particular $D$ ($0 < D < D^*$):

(1) $h_2 \geq h_1 \geq \sqrt{\zeta}$ (Figure 5a): $CO1$ and $CO3$ not admissible. $CO2$ admissible for $A_0 > A_{01}$ and $CO4$ admissible for $A_0 > A_{02}$.

(2) $h_2 \geq \sqrt{\zeta} \geq h_1$ (Figure 5b): $CO2$ admissible and $CO3$ not admissible. $CO1$ admissible for $\psi(D) \leq A_0 < A_{01}$, and $CO4$ admissible for $A_0 > A_{02}$.

(3) $h_1 \leq h_2 \leq \sqrt{\zeta}$ (Figure 5c): $CO2$ and $CO4$ admissible. $CO1$ admissible for $\psi(D) \leq A_0 < A_{01}$, and $CO3$ admissible for $\psi(D) \leq A_0 < A_{02}$.

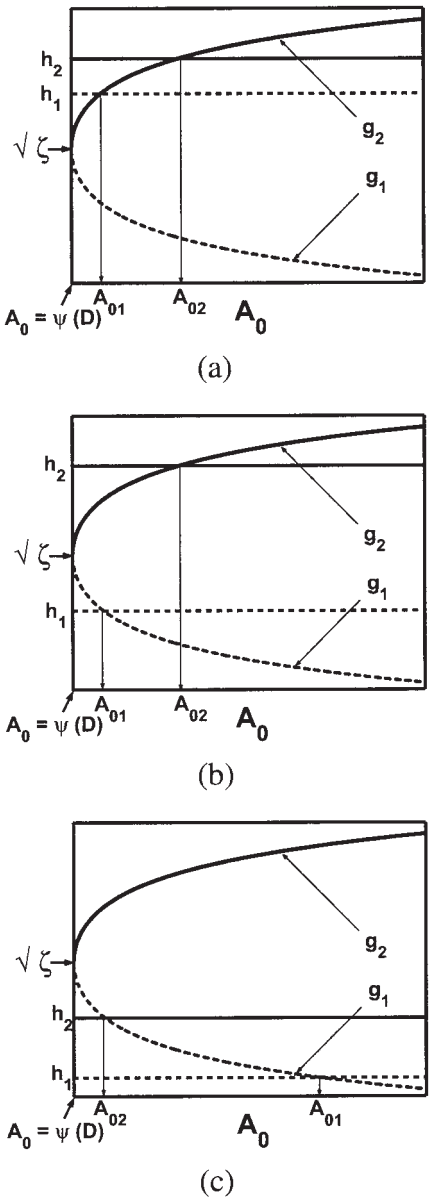


**Figure 5. Dispositions of profiles of $g_1$ (dashed curve), $g_2$ (solid curve), $h_1$ (dashed horizontal line), and $h_2$ (solid horizontal line) for fixed $D$.**

Parts (a), (b), and (c) pertain to 1. $h_2 > h_1 \geq \sqrt{\zeta}$, 2. $h_2 > \sqrt{\zeta} > h_1$, and 3. $h_1 < h_2 \leq \sqrt{\zeta}$, respectively.

Note that $A_{01} = A_{02}$ when $h_1 = h_2$, which occurs when $D = D^*$.

For the kinetic parameters under consideration (Table 1), profiles of $(h_1 - \sqrt{\zeta})$ and $(h_2 - \sqrt{\zeta})$ *vs.* $D$ are provided in Figure 6. For $0 < D < D_2$ ($D_2 = 3.501157 \times 10^{-6}\ \text{s}^{-1}$), $h_2 > \sqrt{\zeta} > h_1$, and, therefore, conclusions in (2) are applicable. For $D_2 \leq D \leq D^*$ ($D^* = 3.5162 \times 10^{-6}\ \text{s}^{-1}$), $h_1 \leq h_2 \leq \sqrt{\zeta}$, and conclusions in (3) are applicable. The profiles of $A_{01}$ and $A_{02}$ *vs.* $D$ shown in Figure 7 enable us to divide the portion of the $(D, A_0)$ space where steady-state coexistence is possible into different regions based on diversity of coexistence steady states. The profiles of $A_{01}$ and $A_{02}$ intersect at $D = D_1$ ($D_1 = 3.22106 \times 10^{-6}\ \text{s}^{-1}$), and $D = D^*$ ($D^* = 3.5162 \times$

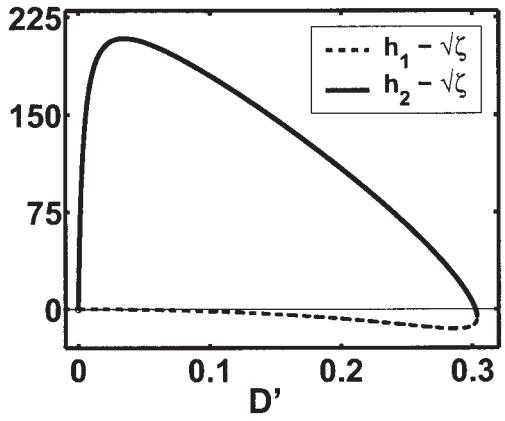


**Figure 6. Profiles of ($h_1 - \sqrt{\zeta}$), dashed curve, and ($h_2 - \sqrt{\zeta}$), solid curve, *vs. D′*.**

$D' = 8.64 \times 10^4 D$ ($D$ in $s^{-1}$, $D'$ in $day^{-1}$), $h_1 < \sqrt{\zeta}$ for $0 < D < D^*$, $h_2 > \sqrt{\zeta}$ for $0 < D < D_2$, $h_2 = \sqrt{\zeta}$ at $D = D_2$, and $h_2 < \sqrt{\zeta}$ for $D_2 < D < D^*$, $D_2 = 3.50116 \times 10^{-6}\ s^{-1}$ and $D^* = 3.5162 \times 10^{-6}\ s^{-1}$.

$10^{-6}\ s^{-1}$), and the profiles of $A_{02}$ and $\psi(D)$ are tangential to one another at $D = D_2$ ($D_2 = 3.501157 \times 10^{-6}\ s^{-1}$).

For $0 < D \leq D_1$, the operating parameter space is divided into four regions depending on which coexistence steady states are admissible (region numbers indicated in parentheses): (1) $A_0 = \psi(D) - CO1$, (2) $\psi(D) < A_0 < A_{01} - CO1, CO2$, (3) $A_{01} \leq A_0 \leq A_{02} - CO2$, and (4) $A_0 > A_{02} - CO2, CO4$. For $D_1 < D < D_2$, the operating parameter space is divided into the following regions: (1) $A_0 = \psi(D) - CO1$, (2) $\psi(D) < A_0 \leq A_{02} - CO1, CO2$, (5) $A_{02} < A_0 < A_{01} - CO1, CO2, CO4$, and (4) $A_0 \geq A_{01} - CO2, CO4$. For $D = D_2$, the interval $A_0 \geq \psi(D)$ is divided into three regions: (1) $A_0 = \psi(D) - CO1$, (5) $\psi(D) \leq A_0 < A_{01} - CO1, CO2, CO4$, and (4) $A_0 \geq A_{01} - CO2, CO4$. For $D_2 < D < D^*$, the operating parameter space is divided into four regions: (6) $A_0 = \psi(D) - CO1, CO3$, (7) $\psi(D) < A_0 < A_{02} - CO1, CO2, CO3, CO4$, (5) $A_{02} \leq A_0 < A_{01} - CO1, CO2, CO4$, and (4) $A_0 \geq A_{01} - CO2, CO4$. For $D = D^*$ ($A_{01} = A_{02}$), the vertical line is divided into three regions: (8) $A_0 = A_0^* - CO3$, (9) $A_0^* < A_0 < A_{01} - CO3, CO4$, and (10) $A_0 \geq A_{01} - CO4$. Since $\bar{C}_2 > C_2$ ($Y_4 > 0$), and $C_1 < C_m$ for $(D, A_0)$ in regions 4, 5, and 7, it follows from the conditions in Eqs. A13 and A19 that stability (instability) of $CO2$ implies stability (instability) of $PW2$ and existence of cyclic state associated with $CO2$ implies existence of cyclic state associated with $PW2$. Since $C_1 < \bar{C}_2 \leq C_2$ in regions 2 and 3 ($Y_2 > 0$), it follows from the conditions in Eq. A13 that $PW2$ is unstable in these regions. Retention of $X$ in a continuous culture at large ($t \to \infty$) then implies retention of $Y$, provided it is present initially in the culture. Among the four coexistence steady states, $CO2$ is the only possibly stable steady state, and it is also the most productive. For these reasons, operation in regions 2–5 and 7 is of interest. Operation in regions 1, 6, and 8–10 is not of interest since stable coexistence is not possible in any of these.

## General Observations on Dynamic Behavior at Large

Among the seven steady states that may be physically realizable, the total washout steady state ($TW$) is locally, asymptotically stable and only two other, $PW2$ and $CO2$, *may be* locally, asymptotically stable. We consider here the transient operation of the mixed culture with fixed operating conditions (fixed $D$ and $A_0$). The two-dimensional (2-D) operating parameter ($D$, $A_0$) space can be divided into three regions: (1) $A_0 \leq \psi(D)$, (2) $A_0 > \psi(D)$, $0 < D < D^*$, and (3) $A_0 > \psi(D)$, $D^* \leq D < (\mu_{1m} - k_1)$ (Figure 3). Retention of $Y$ in the large ($t \to \infty$) is not possible in regions (1) and (3) due to the absence of stable $CO2$ or a stable cyclic state associated with it. These regions, therefore, are not interest to us, since operation in these regions is wasteful. In region 2, retention of $Y$ in the large requires admissibility of a locally stable $CO2$, and/or a locally stable cyclic state associated with it. A prerequisite for this is the retention of $X$ at large $t$. In the ($A$, $B$, $X$) space, the projections of steady states $CO1$, $CO3$, and $PW1$ lie at the same point, and similarly, the projections of steady states $CO2$, $CO4$, and $PW2$ lie at the same point (Table 2), provided of course that the appropriate coexistence steady states are physically realizable. If cyclic states are associated with both $CO2$ and $PW2$, the projections of these in the ($A$, $B$, $X$) space will also be identical. Local stability of $TW$ guarantees a region of attraction for it in the ($A$, $B$, $X$) space.

Stability of either $CO2$, and/or existence of a stable cyclic state associated with it implies existence of a separatrix that divides the ($A$, $B$, $X$) space into (1) basin of attraction of $TW$ (region A), and (2) basin of attraction for retention of $X$ in the reactor (region B) (Figures 8a–8c). The possibilities of interest are: (1) stable $CO2$ without associated cyclic states, (2) unstable $CO2$ with a stable cyclic state associated with it, (3) stable

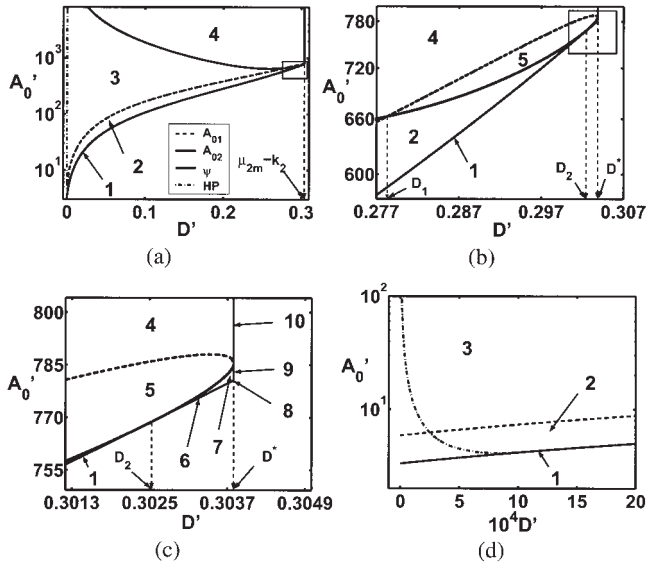


**Figure 7. Division of the operating parameter, ($D$, $A_0$), space into multiple regions based on admissibility of the four coexistence steady states.**

$A_0' = 10^3 A_0$, $D' = 8.64 \times 10^4 D$ ($A_0$ in $kg/m^3$, $A_0'$ in $mg/dm^3$, $D$ in $s^{-1}$, $D'$ in $day^{-1}$). In each part, the lower solid curve represents $\psi(D)$, the dashed curve the profile of $A_{01}$, and the upper solid curve the profile of $A_{02}$. The profiles of $A_{01}$ and $A_{02}$ intersect at $D = D_1 = 3.22106 \times 10^{-6}\ s^{-1}$, and at $D = D^*$ (part b), and the profiles of $\psi$ and $A_{02}$ touch one another at $D = D_2 = 3.50116 \times 10^{-6}\ s^{-1}$ (part c). (b) provides an enlarged view of the boxed portion in (a), (c) provides an enlarged view of the boxed portion in (b), and (d) provides an enlarged view of the portion in (a) near the locus of Hopf points (HP). The numbers refer to regions described in the text. The curve - · - · - in (a) and (d) denotes the locus of Hopf bifurcation points.

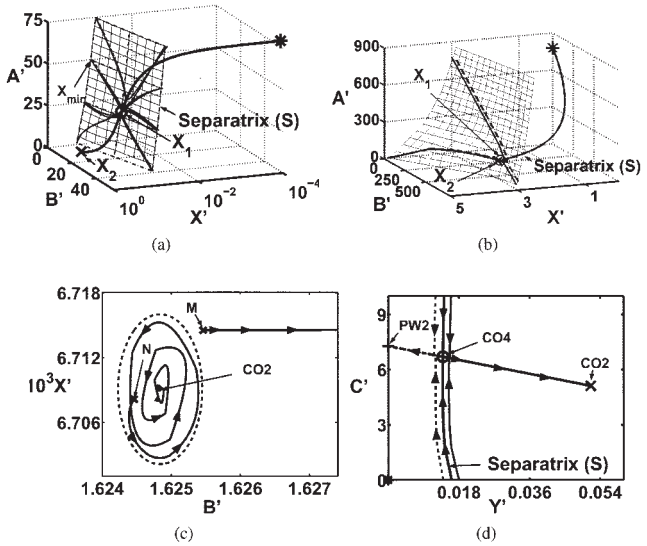


**Figure 8. Division of concentration spaces for subsystems I and II into basins of attraction of locally stable states.**

$J' = 10^3 J$, $J = A, B, C, X, Y$. (a), (b). Division of ($A$, $B$, $X$) space into regions where $X$ is washed out (region A, $TW$ indicated by *) and $X$ is retained (region B, projection of $PW2$, $CO2$, and $CO4$ indicated by x and $X_2$) for (a) $D = 4.63 \times 10^{-7}$ s$^{-1}$ and $A_0 = 0.05$ kg/m$^3$ ($PW2$ unstable), and (b) $D = 3.50926 \times 10^{-6}$ s$^{-1}$ and $A_0 = 0.775$ kg/m$^3$ ($PW2$ stable). In each part, the net represents the separatrix for subsystem $I$, which passes through the projection of $PW1$, $CO1$, and $CO3$ (indicated by ○). Cyclic states are not associated with $CO2$ in either case. In (a), starting with a mixed culture at $A(0) = A_0$, $B(0) = C(0) = 0$, $X(0)$ must exceed $X_{min}$ for long-term retention of $X$. (c). Division of ($A$, $B$, $X$) space into regions, where $X$ is washed out (region A, lying outside the unstable limit cycle indicated by dashed curve), and $X$ is retained (region B, lying inside the unstable limit cycle, projection of $PW2$, $CO2$, and $CO4$ indicated by arrow) for $D = 2.461 \times 10^{-10}$ $s^{-1}$ and $A_0 = 0.05$ kg/m$^3$ ($PW2$ unstable). For the sake of clarity, only projections in the ($B$, $X$) plane are shown. Trajectories starting at $M$ and $N$ lead eventually to $TW$ and $CO2$, respectively. (d). Division of ($C$, $Y$) plane into regions, where $Y$ is retained (region C) and $Y$ is washed out (region D) for reactor operations started in region B (long-term retention of $X$) of the ($A$, $B$, $X$) space in (b) [$D = 3.50926 \times 10^{-6}$ s$^{-1}$, $A_0 = 0.775$ kg/m$^3$]. $CO2$ and $PW2$ are locally stable with no cyclic states associated with these. The separatrix which separates region C from region D passes through the projection of $CO4$ on this plane.

$CO2$ with a stable cyclic state associated with it, and (4) stable $CO2$ with only an unstable cyclic state associated with it. For the first three possibilities, since $CO1$, $CO3$, and $PW1$ are unstable and have the same projection, a point, in the ($A$, $B$, $X$) space ($X = X_1$), with $0 < X_1 < X_2$, the separatrix must pass through this point (Figures 8a and 8b). Region B is the projection in the ($A$, $B$, $X$) space of the basin of attraction of (1) locally stable $CO2$ if no cyclic states are associated with $CO2$ (possibility 1), or (2) a stable cyclic state associated with $CO2$ if $CO2$ is unstable (possibility 2). If a stable $CO2$ and a stable cyclic state associated with it exist (possibility 3), then region B is divided further into basins of attraction of $CO2$ (region B1), and the locally stable cyclic state associated with $CO2$ (region B2), by an unstable cyclic state (serving as the separatrix) that lies between the two locally stable states. If only an unstable cyclic state is associated with a stable $CO2$ (possibility 4), then the projection of the unstable cyclic state in the ($A$, $B$, $X$) space serves as the separatrix (Figure 8c). The portion of the ($A$, $B$, $X$) space lying outside the projection of the unstable cyclic state in this space then constitutes region A, and the portion of the ($A$, $B$, $X$) space lying inside the projection of the cyclic state in this space constitutes region B. For each possibility, the initial reactor state must lie in region B for long-term retention of $X$. It must be realized that a continuous culture operation is normally preceded by a batch or fed-batch culture. The initial reactor state for continuous culture operation then corresponds to the final state of the batch or fed-batch operation that precedes it.

Next, we look at when $Y$ is retained in the reactor for reactor operations started in the region B of the ($A$, $B$, $X$) space. If $PW2$ is unstable and does not have a locally stable cyclic state associated with it (regions 2 and 3 of the ($D$, $A_0$) space defined in the previous section and Figure 7), retention of $Y$ in the culture is guaranteed. If a cyclic state associated with a locally stable $CO2$ is not admissible (possibility 1) or if only an unstable cyclic state is associated with a stable $CO2$ (possibility 4), all trajectories eventually must lead to $CO2$ (Figures 8a and 8c). If a locally stable cyclic state associated with unstable $CO2$ is admissible (possibility 2), all trajectories eventually must lead to the cyclic state. If a locally stable cyclic state associated with a locally stable $CO2$ is admissible (possibility 3), the ($C$, $Y$) space is divided into basins of attraction of $CO2$, and the locally stable cyclic state associated with it, an unstable cyclic state that lies between the two states serving as the separatrix.

When at least $CO2$ or a cyclic state associated with it is locally stable and the same is the situation with $PW2$ (possible only if $CO4$ is admissible, regions 4, 5, and 7 of the ($D$, $A_0$) space defined in the previous section and Figure 7), the ($C$, $Y$) space is divided into regions C and D, which are the domains of reactor trajectories which lead to retention of $Y$ and washout of $Y$, respectively. The separatrix that divides the ($C$, $Y$) space passes through the projection of $CO4$ in this space (Figure 8d). Whether the culture remains mixed (both $X$ and $Y$ retained) or becomes pure (only $X$ retained), depends on where $C$ and $Y$ are once $A$, $B$ and $X$ have converged to the projections of the steady states $CO2$ and $PW2$ or the cyclic state associated with these steady states in the ($A$, $B$, $X$) space. Retention of $Y$ requires that $C$ and $Y$ lie in region C at this stage. If a unique stable coexistence state ($CO2$ or cyclic state associated with it) exists (possibilities 1, 2, and 4), all trajectories of $C$ and $Y$ will converge to it in region C. If a locally stable cyclic state associated with a stable $CO2$ is admissible (possibility 3), region C is divided into basin of attraction of $CO2$, region C1, and basin of attraction of the locally stable cyclic state associated with $CO2$, region C2, with an unstable cyclic state that lies between the two states serving as the separatrix.

For the kinetic parameter values under consideration, possibilities 2 and 3 are not encountered for all values of $D$ and $A_0$.

## Specific Results

For a particular $A_0$, let $D_m$ denote the maximum dilution rate for which coexistence is possible. It is evident from Figure 3 that for $A_0 \leq \psi(D^*)$, $D_m$ satisfies the relation $A_0 = \psi(D_m)$ and $D_m = D^*$ for $A_0 \geq \psi(D^*)$. The profile of $D_m$ is shown in Figure 9a. In the profiles of $X$ and $Y$ for coexistence and partial washout steady states that will be presented in what

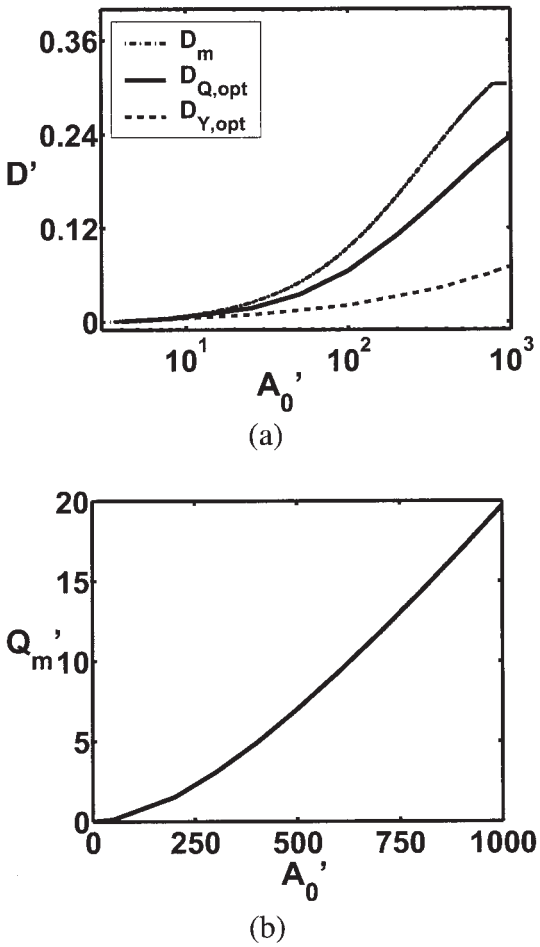


**Figure 9. Variations in (a) $D_m$ (solid curve), $D_{Q,opt}$, optimum $D$ for maximum $Q$ (maximum $Q_2$, thick solid curve), and $D_{Y,opt}$, optimum $D$ for maximum $Y$ (maximum $Y_2$, dashed curve), and (b) maximum $Q$, $Q_{max}$ with variation in $A_0$. $A_0' = 10^3 A_0$, $D' = 8.64 \times 10^4 D$ and $Q_m' = 8.64 \times 10^7 Q_{max}$. $A_0$ is in kg/m$^3$, $A_0'$ in mg/dm$^3$, $D$ in s$^{-1}$, $D'$ in day$^{-1}$, $Q_{max}$ in m$^3$/s, and $Q_m'$ in dm$^3$/day.**

follows, the solid curves will denote stable steady states, and the dashed curves will represent unstable steady states. Since $B$, $C_1$ and $C_2$ are dependent only on $D$ (Eqs. 12 and 13), the profiles of these can be deduced from Figure 2. The profile of $A$ *vs.* $D$ can be readily obtained from the profile of $X$ *vs.* $D$, because of the one-to-one correspondence between $A$ and $X$ (Eq. 14). For these reasons, profiles of $A$, $B$ and $C$ for variable $D$ are not shown here.

The steady states for a specific set of operating parameters were identified using MAPLE 9.[29] The bifurcation diagrams were obtained using the continuation toolbox CL_MATCONT 1.1[30] for MATLAB 6.5.[31] The software allows for tracing of steady state and periodic solutions, and locating various bifurcation points, such as limit and Hopf points.

For $\psi(D) \le A_0 \le A_{01}$ $(D_1)$ $(D_1 = 3.22106 \times 10^{-6}\ \mathrm{s}^{-1})$, $CO2$ is always admissible, while $CO1$ is admissible only in regions 1 and 2 and $PW2$ is unstable (Figures 7a and 7b). For the parameter values listed in Table 1, $CO2$ is subject to Hopf bifurcation. The locus of Hopf points is represented by the curve HP in Figures 7a and 7d and exhibits a minimum $A_0$. Let $A_{0c}$ denote this minimum and $D_c$ the corresponding $D$. For the parameter values under consideration, $A_{0c} = 4.10385 \times 10^{-3}$ kg/m$^3$ and $D_c = 1.0044 \times 10^{-8}\ \mathrm{s}^{-1}$. For $0 < A_0 < A_{0c}$, $CO2$ is unstable wherever admissible (Figure 10a). For $A_0 = A_{0c}$, two eigenvalues of **A** (Eq. A2) are imaginary at $D = D_c$ and complex with positive real parts for other $D$ in the immediate neighborhood of $D = D_c$. Crossover of the imaginary axis by the two eigenvalues as $D$ is increased (decreased) does not occur at $D_c$. As a result, $CO2$ is unstable at every $D$ $(0 < D \le D_m)$, and the operating point $(D_c, A_{0c})$ is the point of emergence of Hopf bifurcation. In the immediate vicinity of $A_{0c}$ with $A_0 > A_{0c}$, $CO2$ undergoes Hopf bifurcation at two values of $D$, $D_{H1}$ and $D_{H2}$ $(D_{H2} > D_{H1})$. $CO2$ is unstable for $0 < D \le D_{H1}$ and $D_{H2} \le D \le D_m$, and stable for $D_{H1} < D < D_{H2}$ (Figure 10b). The two Hopf bifurcation points, $D_{H1}$ and $D_{H2}$, diverge rapidly as $A_0$ is increased. Hopf bifurcation occurs at two dilution rates over a very narrow range of $A_0$,

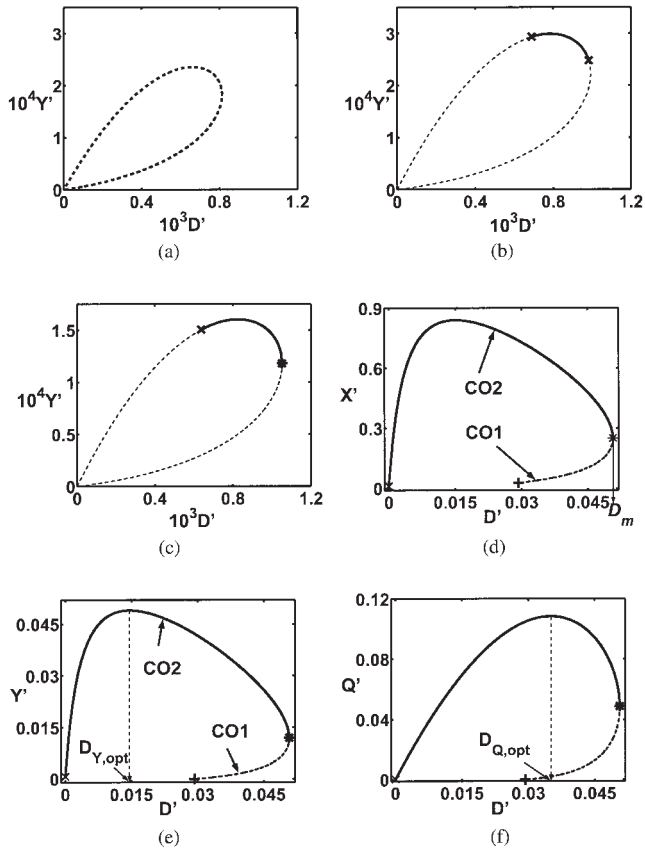


**Figure 10. Profiles of $Y'$ *vs.* $D'$ for (a) $A_0 = 4 \times 10^{-3}$, (b) $A_0 = 4.15 \times 10^{-3}$, (c) $A_0 = 4.2029 \times 10^{-3}$, and (e) $A_0 = 0.05$, and profiles of (d) $X'$ and (f) $Q'$ *vs.* $D'$ for $A_0 = 0.05$. ($X' = 10^3 X$, $Y' = 10^3 Y$, $D' = 8.64 \times 10^4 D$, $Q' = 8.64 \times 10^7 Q$, $A_0$, $X$, and $Y$ in kg/m$^3$, $D$ in s$^{-1}$, and $Q$ in m$^3$/s.)**

The solid and dashed curves indicate stable and unstable steady states, respectively. In each part, the lower portion of the curve represents $CO1$, and the upper portion $CO2$. $*$ and $\times$ denote the static and Hopf bifurcation points, respectively, for $CO2$ and $+$ in (d–f) denotes the emergence of $CO1$ from $PW1$.

$A_{0c} < A_0 < A_{03}$, with $A_{03} = 4.20295 \times 10^{-3}$ kg/m$^3$. The Hopf bifurcation at the higher dilution rate disappears as $A_0 \to A_{03}$ since $D_{H2} \to D_m$ (Figure 10c). For $A_0 \geq A_{03}$, Hopf bifurcation occurs at only one $D$, $D_{H1}$, $D_{H1}$ being very low, with the locus of the Hopf points lying entirely in region 3 (Figure 7a). It was established earlier that $CO2$ is unstable in the vicinity of $D = 0$. The occurrence of Hopf bifurcation at $D = D_{H1}$ for $A_0 > A_{0c}$ is consistent with that result. For $0 < D \leq D_{H1}$ and $D_{H2} \leq D \leq D_m$, where applicable, $CO2$ is unstable and retention of $X$ and $Y$ is not possible ($TW$ globally stable). The Hopf bifurcations at $D = D_{H1}$ for $A_0 > A_{0c}$, and at $D = D_{H2}$ for $A_{0c} < A_0 < A_{03}$ are *subcritical,* with an unstable periodic state (limit cycle) surrounding the stable $CO2$ (possibility 4 discussed in the previous section). The limit cycles exist in only a small neighborhood of each bifurcation point, and are characterized by very small amplitudes, and very low frequencies (very large periods). Where admissible, the projection of the unstable limit cycle in the ($A$, $B$, $X$) space serves as the separatrix for basins of attraction of $TW$ and $CO2$ (Figure 8c). In the portion of the interval $D_{H1} < D < D_{H2}$ for $A_{0c} < A_0 < A_{03}$ and $D_{H1} < D < D_m$ for $A_{03} \leq A_0 \leq A_{01}$ ($D_1$), where $CO2$ is stable and an unstable limit cycle does not surround it, the separatrix for basins of attraction of $TW$ and $CO2$ passes through the projection of $PW1$ in the ($A$, $B$, $X$) space (possibility 1 discussed in the previous section, Figure 8a). This is also the case for regions 2 and 3, where admissible, for $A_0 \geq A_{01}(D_1)$. Both $PW2$ and $CO2$ are locally, asymptotically stable in regions 4, 5, and 7 of the ($D$, $A_0$) space (Figure 7). The separatrix for basins of attraction of $TW$ and $CO2/PW2$ then passes through the projection of $PW1$ in the ($A$, $B$, $X$) space (Figure 8b). The ($C$, $Y$) plane is divided into regions of attraction of $CO2$ and $PW2$ by a separatrix which passes through the projection of $CO4$ on this plane (Figure 8d). In the range $A_{03} \leq A_0 \leq A_{01}(D_1)$, the profiles of $X$, $Y$, and $Q$ for different $A_0$ are qualitatively similar (see Figures 10d–10f), with an increase in $D$ leading to the following transition sequence in terms of region numbers: $3 \to 2 \to 1$ (Figure 7). The profile of $Y$ in Figure 10e for $A_0 = 0.05$ kg/m$^3$ indeed reveals these transitions. The profiles of $X$, $Y$, and $Q$ for $CO2$ exhibit maxima at intermediate dilution rates. Since $\mu_2$ increases linearly with increasing $D$ (Eq. 11) one can observe from Eq. 7 that at the optimum $D$ corresponding to maximum $Q$, $Y$ must decrease with increasing $D$. The optimum $D$ at which $Q$ is maximized is, therefore, greater than the optimum $D$ at which $Y$ is maximized (Figures 9a, 10e, and 10f). Further, the maximum $Q$ is attained at a dilution rate less than that corresponding to the limit point for $CO2$, $D_m$ (Figure 9a). For this reason, as stated earlier, reactor operation leading to scenarios 15–17, 20, and 23–25 in Table 3 and in regions 1, 6, and 8–10 of Figure 7, by stabilization of an unstable coexistence steady state using a feedback controller, is not of interest.

In the range $A_{01}(D_1) < A_0 < A_{02}(D_2)$, an increase in $D$ leads to the following transition sequence in terms of region numbers: $3 \to 4 \to 5 \to 2 \to 1$ (Figure 7). The profiles of $Y$ in Figure 11a for $A_0 = 0.7$ kg/m$^3$ indeed reveal these transitions. For $A_0 = A_{02}(D_2)$, an increase in $D$ leads to the following transition sequence in terms of region numbers: $3 \to 4 \to 5 \to 1$. In the range $A_{02}(D_2) < A_0 < A_0^*$, an increase in $D$ leads to the following transition sequence in terms of region numbers: $3 \to 4 \to 5 \to 7 \to 6$ (Figure 7). The profiles of $Y$ in Figure 11b for $A_0 = 0.775$ kg/m$^3$ reveal these transitions. As $A_0$ approaches $A_0^*$, the limit points for the steady-state pairs (1) $CO1$ and $CO2$ and (2) $CO3$ and $CO4$ approach each other and collide when $A_0 = A_0^*$ (Figure 11c, $A_0 = 0.780658$ kg/m$^3$). For $A_0 = A_0^*$, an increase in $D$ leads to the following transition sequence in terms of region numbers: $3 \to 4 \to 5 \to 8$ (Figure 11c). A further increase in $A_0$ leads to switching of the pairs among the four coexistence steady states in a close neighborhood of ($D^*$, $A_0^*$), with the two limit points now corresponding to steady-state pairs (1) $CO1$ and $CO3$, and (2) $CO2$ and $CO4$ (Figure 11d for $A_0 = 0.781$ kg/m$^3$). In the range $A_0^* < A_0 < A_{02}(D^*)$, an increase in $D$ leads to the following transition sequence in terms of region numbers: $3 \to 4 \to 5 \to 7 \to 9$ (Figure 7). The profiles of $Y$ in Figure 11e for $A_0 = 0.786$ kg/m$^3$ reveal these transitions. Finally, for $A_0 > A_{02}(D^*)$, an increase in $D$ leads to the following transition sequence in terms of region numbers: $3 \to 4 \to 10$ (Figure 7). The profiles of $Y$ in Figure 11f for $A_0 = 0.8$ kg/m$^3$ reveal these transitions.

The profiles of optimum $D$ that lead to maximum $Y_2$ and $Q_2$, $Q$ for $CO2$, are shown in Figure 9a, and the profile of maximum $Q_2$ is provided in Figure 9b, $A_0$ being the variable

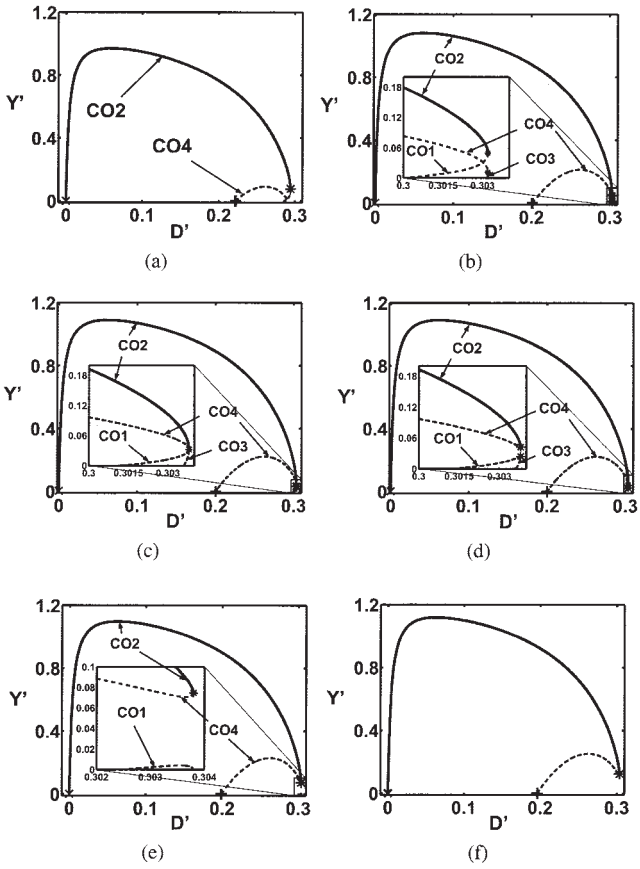


**Figure 11. Profiles of $Y'$ *vs.* $D'$ for (a) $A_0 = 0.7$, (b) $A_0 = 0.775$, (c) $A_0 = 0.780658$, (d) $A_0 = 0.781$, (e) $A_0 = 0.786$, and (f) $A_0 = 0.8$ ($Y' = 10^3 Y$, $D' = 8.64 \times 10^4 D$, $A_0$ and $Y$ in kg/m$^3$, and $D$ in s$^{-1}$.)**

The solid curves denote profiles for $CO2$ (stable) and dashed curves denote profiles for the unstable coexistence steady states. $*$ denotes the static bifurcation point for $CO2$ and $+$ the static bifurcation point for $PW2$ (emergence of $CO4$).

parameter. Since $Q_2 = \varepsilon(k_2 + D)Y_2$, in view of Eqs. 17, 20, 21, and 24 it can be deduced that

$$\frac{\partial Q_2}{\partial A_0} = \frac{\varepsilon\gamma}{2\alpha\beta\delta}\frac{\partial g_2}{\partial A_0} > 0 \tag{26}$$

The maximum $Q_2$ ($Q_{max}$), thus, increases with increasing $A_0$ (Figure 9b).

The use of the unstructured kinetic model in this study has been based on availability of all kinetic parameters in it and its wide applicability in the prior literature for prediction of operation of anaerobic digesters. With the growth in the experimental database, fully determined (vis-a-vis kinetic parameters) kinetic models with more mechanistic detail will become available. These will account for more biological species (more interaction) and chemical species (more structure), and as a result, will be more robust than the model considered here. These models can be subjected to similar analysis. In this study, only a binary interaction, commensalism, was considered since only two groups of microorganisms were considered. In a kinetic model with greater mechanistic detail, the steady-state characteristics and structure will be considerably different and much richer owing to an increase in the number and type of interactions among the biological species, and consideration of much higher number of chemical species and chemical reactions. These issues will be pursued in future studies.

## Conclusions

Steady state and dynamic behavior of a continuous commensalistic culture with kinetic feedback has been analyzed and investigated in detail. A three-stage process concerning anaerobic digestion of complex insoluble organics by a consortium of acid generating bacteria (host cell species) and methane generating bacteria (commensal cell species), has been considered as the example process. Based on retention of one or both cell species, steady states have been classified into three types, only one type, coexistence of both cell species, being of interest for completion of the process. For the form of the kinetics considered, the reactor can operate at up to seven steady states, the omnipresent total washout state, up to two partial washout states, and up to four coexistence states. Criteria for admissibility and local stability of different steady states have been derived analytically. While the total washout state is universally locally stable, at the most one coexistence steady state may be locally stable. Bifurcation characteristics of the coexistence and partial washout steady states have been analyzed. For the specific kinetic parameter set under consideration, the operating parameter, ($D$, $A_0$), space is divided into multiple regions based on whether or not the host species or both cell species are retained in the reactor in a steady-state operation. The portion of the ($D$, $A_0$) space where steady-state coexistence is possible is divided further into multiple regions based on which of the four coexistence steady states are admissible. The dynamic characteristics of the reaction system have been investigated for transient operations of the mixed culture with fixed operating conditions to identify basins of attraction of the candidate locally stable steady states and suggest startup policies to reach the desired coexistence steady state. Among the four coexistence steady states possible, the specific synthesis rate of the target product, biogas, is highest for the only locally stable steady state. Admissibility of cyclic states via Hopf bifurcation has been investigated. For the kinetic parameter set under consideration, unstable limit cycles arise at very low $D$ and $A_0$ and in a very narrow, $A_0$ range in a small neighborhood of the Hopf bifurcation points. These limit cycles have very small amplitudes and very large periods. Numerical results illustrate bifurcation patterns of the coexistence steady states, and how various coexistence steady states emerge and disappear as the operating parameters are varied. The entire analysis has been facilitated by kinetics-based compartmentalization of the process.

## Notation

$A, B, C, X, Y$ = concentrations of $A$, $B$, $C$, $X$, and $Y$, respectively, kg/m$^3$
$a, b$ = defined in Eq. 20
$A_0$ = concentration of $A$ in the feed, kg/m$^3$
$A_0^*$ = $=\psi(D^*)$, kg/m$^3$
$a_1, a_2, a_3$ = defined in Eq. A10
$A_{01}$ = $A_0$ corresponding to intersection of $h_1$ and $g_1$ or $g_2$, kg/m$^3$
$A_{02}$ = $A_0$ corresponding to intersection of $h_2$ and $g_1$ or $g_2$, kg/m$^3$
$\mathbf{A}, \mathbf{B}, \mathbf{C}, \mathbf{D}$ = defined in Eqs. A2 and A3
$A, B, C$ = complex insoluble organics, soluble organics, and volatile acids, respectively
$b_1$ = defined in Eq. A11
$\bar{C}_1, \bar{C}_2$ = $\bar{C}$ corresponding to $X_1$ and $X_2$, respectively, defined in Eq. 21, kg/m$^3$
$\bar{C}$ = defined in Eq. 19, kg/m$^3$
$C_1, C_2$ = defined in Eq. 13, kg/m$^3$
$C_m$ = concentration of $C$ corresponding to maximum $\mu_2$, defined in Eq. 9, kg/m$^3$
$CO$ = coexistence steady state $X > 0$, $Y > 0$
$CO_j$ = coexistence steady states with notation in Table 2, $j$ = 1–4
$D$ = dilution rate ($=q_0/V$), s$^{-1}$
$D^*$ = $=(\mu_{2m} - k_2)$, s$^{-1}$
$det$ = determinant
$E$ = extracellular enzymes synthesized by $X$
$f_1 - f_5$ = defined in Eqs. 2–6
$g_1, g_2, h_1, h_2$ = defined in Eq. 24
$j_{pq}$ = element of $\mathbf{J}$ in row $p$ and column $q$, $p, q$ = 1–5, defined in Eq. A3 when non-zero
$\mathbf{J}$ = Jacobian matrix defined in Eqs. A1–A3
$k_1, k_2$ = death-rate coefficients for acidogens and methanogens, respectively, s$^{-1}$
$K_1, K_2$ = saturation constants in growth rate expressions (Eq. 8) for acidogens and methanogens, respectively, kg/m$^3$
$K_I$ = inhibition coefficient in the growth rate expression for methanogens in Eq. 8, kg/m$^3$
$P$ = biogas (metabolites produced by $Y$)
$PW$ = partial washout steady-state, $X > 0$, $Y = 0$
$PW_j$ = partial washout steady states with notation in Table 2, $j$ = 1, 2
$Q$ = biogas production rate, defined in Eq. 7, m$^3$/s
$q_0$ = volumetric feed and effluent flow rate, m$^3$/s
$Q_2$ = $Q$ for $Y = Y_2$ ($CO2$), m$^3$/s
$r_1$ = rate of first step in Eq. 1, defined in Eq. 8, kg/{m$^3$ · s}
$t$ = real time, s
$tr$ = trace
$TW$ = total washout steady state, $X = Y = 0$
$V$ = culture volume, m$^3$
$X_1, X_2$ = defined in Eq. 17
$X, Y$ = acidogens and methanogens, respectively
$Y_j$ = $Y$ for $CO_j$, $j$ = 1–4 provided in Eq. 21
$\alpha$ = kinetic parameter in expression for $r_1$ in Eq. 8, m$^3$/{kg X · s}

$\beta$ = yield coefficient for soluble organics utilized by acidogens, kg B/kg $X$
$\Delta$ = defined in Eq. 17
$\delta$ = yield coefficient for utilization of volatile acids by methanogens, kg C/kg $Y$
$\varepsilon$ = yield coefficient for biogas produced by methanogens, $\{m^3\ P\}\{m^3\ culture\}$/kg $Y$
$\gamma$ = yield coefficient for volatile acids produced by acidogens, kg $C$/kg $X$
$\lambda$ = eigenvalue of $\mathbf{J}$
$\mu_{10}$, $\mu_{20}$ = parameters in Eq. 8, $s^{-1}$
$\mu_{1B}$ = derivative of $\mu_1$ with respect to $B$
$\mu_{1m}$, $\mu_{2m}$ = maximum specific growth rates of acidogens and methanogens, respectively, defined in Eq. 9, $s^{-1}$
$\mu_1$, $\mu_2$ = specific growth rates of acidogens and methanogens, respectively, $s^{-1}$
$\mu_{2C}$ = derivative of $\mu_2$ with respect to $C$
$\nu$, $\xi$ = defined in Eq. 13
$\phi$ = defined in Eq. 16
$\psi(D)$ = defined in Eq. 18
$\rho(X_1)$, $\rho(X_2)$ = defined in Eq. A12
$\zeta$ = defined in Eq. 24

## Literature Cited


1. Fredrickson AG, Tsuchiya HM. Microbial Kinetics and Dynamics. In: Lapidus L, Amundson NR, eds. *Chemical Reactor Theory, A Review.* Englewood Cliffs, NJ: Prentice Hall; 1977.
2. Bailey JE, Ollis DF. *Biochemical Engineering Fundamentals.* 2nd ed. New York City, NY: McGraw-Hill; 1986.
3. Bungay HR, Bungay ML. Microbial interactions in continuous culture. *Adv Appl Microbiol.* 10:269–290;1968.
4. Shuler ML, Kargi F. *Bioprocess Engineering: Basic Concepts.* 2nd ed. Englewood Cliffs, NJ: Prentice Hall; 2002.
5. Parulekar SJ, Lim HC. Dynamics of continuous commensalistic cultures—I. Multiplicity and local stability of steady states and bifurcation analysis. *Chem Eng Sci.* 41:2605–2616;1986.
6. Zeikus G, Johnson EA, eds. *Mixed Cultures in Biotechnology.* New York City, NY: McGraw-Hill; 1991.
7. Reilly PJ. Stability of commensalistic systems. *Biotechnol Bioeng.* 16:1373–1392;1974.
8. Stephanopoulos G. The dynamics of commensalism. *Biotechnol Bioeng.* 23:2243–2255;1981.
9. Sheintuch M. Dynamics of commensalistic systems with self- and cross-inhibition. *Biotechnol Bioeng.* 22:2557–2577;1980.
10. Parulekar SJ, Lim HC. Dynamics of continuous commensalistic cultures—II. Numerical results for steady-state multiplicity regions and transient behavior in-the-large. *Chem Eng Sci.* 41:2617–2628;1986.
11. Simeonov I, Momchev V, Grancharov D. Dynamic modeling mesophilic anaerobic digestion of animal waste. *Water Res.* 30:1087–1094; 1996.
12. Simeonov I, Stoyanov S. Modeling and dynamic compensator control of the anaerobic digestion of organic wastes. *Chem Biochem Eng Q.* 17(4):285–292;2003.
13. Reith JH, Wijffels RH, Barten H, eds. *Bio-Methane & Bio-Hydrogen: Status and Perspectives of Biological Methane and Hydrogen Production.* Dutch Biological Hydrogen Foundation; 2003.
14. Wheatley AD, ed. *Anaerobic Digestion: A Waste Treatment Technology.* London: Elsevier Applied Science; 1991.
15. Hobson PN, Wheatley AD. *Anaerobic Digestion: Modern Theory and Practice.* London: Elsevier Applied Science; 1992.
16. Karim K, Klasson KT, Hoffmann R, Drescher SR, DePaoli DW, Al-Dahhan MH. Anaerobic digestion of animal waste: effect of mixing. *Bioresource Technol.* Available at: http://www.sciencedirect.com/science/article/B6V24–4FK42H7–3/2/339d67778b61b0e8c9cf83bed45c3568. Accessed March 8, 2005.
17. Bouskova A, Dohanyos M, Schmidt JE, Angelidaki I. Strategies for changing temperature from mesophilic to thermophilic conditions in anaerobic CSTR reactors treating sewage sludge. *Water Res.* 39:1481–1488;2005.
18. Dinsdale RM, Premier GC, Hawkes FR, Hawkes DL. Two-stage anaerobic co-digestion of waste activated sludge and fruit/vegetable waste using inclined tubular digesters. *Bioresource Technol.* 72:159–168;2000.
19. Hill DT, Barth CL. A dynamic model for simulation of animal waste digestion. *J of Water Pollution Control Federation.* 10:2129–2143; 1977.
20. Pahl M, Lunze J. Dynamic modelling of a biogas tower reactor. *Chem Eng Sci.* 53:995–1007;1997.
21. Tartakovsky B, Guiot SR, Sheintuch M. Modeling and analysis of co-immobilized aerobic/anaerobic mixed cultures. *Biotechnol Progr.* 14:672–679;1998.
22. Noykova N, Muller TG, Gyllenberg M, Timmer J. Quantitative analyses of anaerobic wastewater treatment processes: Identifiability and parameter estimation. *Biotechnol Bioeng.* 78:89–103;2002.
23. Keshtkar A, Meyssami B, Abolhamd G, Ghaforian H, Khalagi Asadi M. Mathematical modeling of non-ideal mixing continuous flow reactors for anaerobic digestion of cattle manure. *Bioresource Technol.* 87:113–124;2003.
24. Jeyaseelan S. A simple mathematical model for anaerobic digestion process. *Water Sci. Technol.* 35:185–191;1997.
25. Angelidaki I, Ellagard L, Ahring BK. A comprehensive model of anaerobic bioconversion of complex substrates to biogas. *Biotechnol Bioeng.* 63:363–372;1999.
26. Husain A. Mathematical models of the kinetics of anaerobic digestion—a selected review. *Biomass Bioenergy.* 14:561–571;1998.
27. v. Munch E, Keller J, Lant P, Newell R. Mathematical modelling of prefermenters—I. Model development and verification. *Water Res.* 33:2757–2768;1999.
28. Seborg DE, Edgar TF, Mellichamp DA. *Process Dynamics and Control.* 2nd ed. New York: Wiley; 2004.
29. MAPLE 9 (Waterloo Maple Inc., Ontario, 2003).
30. Dhooge A, Govaerts W, Kuznetsov YA, Mestrom W, Riet AM. CL_MATCONT: a continuation toolbox in Matlab in SAC '03: *Proceedings of the 2003 ACM symposium on applied computing:* 161–166, ACM Press, 2003.
31. MATLAB 6.5, The Mathworks, Inc., http://www.mathworks.com.


## Appendix: Criteria for Stability and Bifurcation of Steady States

The local stability of steady states is determined by the eigenvalues of the Jacobian matrix ($\mathbf{J}$) associated with Eqs. 2–6, $\mathbf{J}$ being

$$\mathbf{J} = \left\{ j_{pq}, j_{pq} = \frac{\partial f_p}{\partial x_q}, p, q = 1, 2, \ldots, 5 \right\}, \quad x_1 = A, \quad x_2 = X, \quad x_3 = B, \quad x_4 = Y, \quad x_5 = C \tag{A1}$$

The expression for $\mathbf{J}$ is

$$\mathbf{J} = \begin{bmatrix} \mathbf{A} & \mathbf{C} \\ \mathbf{D} & \mathbf{B} \end{bmatrix}$$

with

$$\mathbf{A} = \begin{bmatrix} j_{11} & j_{12} & 0 \\ 0 & j_{22} & j_{23} \\ j_{31} & j_{32} & j_{33} \end{bmatrix}, \qquad \mathbf{B} = \begin{bmatrix} j_{44} & j_{45} \\ j_{54} & j_{55} \end{bmatrix}, \qquad \mathbf{C} = \mathbf{0}, \qquad \mathbf{D} = \begin{bmatrix} 0 & 0 & 0 \\ 0 & j_{52} & j_{53} \end{bmatrix} \tag{A2}$$

The nonzero elements of the Jacobian matrix are

$$j_{11} = -(D + \alpha X), \quad j_{12} = -\alpha A, \quad j_{22} = (\mu_1 - k_1 - D), \quad j_{23} = X\mu_{1B}, \quad j_{31} = \alpha X$$

$$j_{32} = (\alpha A - \beta\mu_1), \quad j_{33} = -(D + \beta X\mu_{1B}), \quad j_{44} = (\mu_2 - k_2 - D), \quad j_{45} = Y\mu_{2C}$$

$$j_{52} = \gamma\mu_1, \quad j_{53} = \gamma X\mu_{1B}, \quad j_{54} = -\delta\mu_2, \quad j_{55} = -(D + \delta Y\mu_{2C})$$

$$\mu_{1B} = \frac{d\mu_1}{dB}, \quad \mu_{2C} = \frac{d\mu_2}{dC} \tag{A3}$$

The eigenvalues $\lambda$ of **J** are the roots of the characteristic equation for the same, viz., $\det(\mathbf{J} - \lambda\mathbf{I}) = 0$, with **I** being a $(5 \times 5)$ identity matrix. Triviality of **C** is due to independence of Eqs. 2–4 from $C$ and $Y$. Since **C** is trivial, the characteristic equation for **J** reduces to

$$\det(\mathbf{A} - \lambda\mathbf{I})\det(\mathbf{B} - \lambda\mathbf{I}) = 0 \tag{A4}$$

This finding is not surprising in view of the division of the reactor system into two subsystems depicted in Figure 1. The eigenvalues of **J**, therefore, are the eigenvalues of **A** and **B**. The criteria for local stability of the three steady-state types, total washout, partial washout, and coexistence steady states, are derived next using Eqs. A2–A4. For the total washout steady state, $A = A_0$ and $B$, $C$, $X$, and $Y$ are trivial, and therefore Eq. A4 reduces to

$$(D + \lambda)^3(D + k_1 + \lambda)(D + k_2 + \lambda) = 0 \tag{A5}$$

It is evident that all eigenvalues of **J** are real and negative for $D > 0$ and, therefore, the total washout steady state is locally, asymptotically stable for $D > 0$. For coexistence and partial washout steady states, the characteristic equation for **A** has the same expression, while that for **B** has different expressions. In the following, we work with these characteristic equations to rule out stability of some of the coexistence and partial washout steady states, and obtain the necessary and sufficient conditions for local, asymptotic stability of the remaining ones.

The eigenvalues of **B** are the roots of

$$\lambda^2 - \mathrm{tr}(\mathbf{B})\lambda + \det(\mathbf{B}) = 0, \quad \mathrm{tr}(\mathbf{B}) = (j_{44} + j_{55}), \quad \det(\mathbf{B}) = (j_{44}j_{55} - j_{45}j_{54}) \tag{A6}$$

For stability of a steady state, it is necessary and sufficient that $\mathrm{tr}(\mathbf{B}) < 0$ and $\det(\mathbf{B}) > 0$. For a partial washout steady state, $j_{45} = 0$, and Eq. A6 reduces to

$$(D + \lambda)(\mu_2 - k_2 - D - \lambda) = 0 \Rightarrow \lambda = -D, \quad \lambda = (\mu_2 - k_2 - D) \tag{A7}$$

For stability of a partial washout steady state, it is therefore *necessary* that $\mu_2(\bar{C}) < (D + k_2)$. This condition is obviously satisfied when $\mu_{2m} < (D + k_2)$ since $\mu_2(\bar{C}) \leq \mu_{2m}$. When $(D + k_2) \leq \mu_{2m}$, it should be evident from Figure 2b that the necessary condition for stability of a partial washout steady state ($PW$) is satisfied if $\bar{C} < C_1$ or $\bar{C} > C_2$, and violated if $C_1 \leq \bar{C} \leq C_2$ (unstable $PW$). For a coexistence steady state, satisfaction of Eq. 11 implies triviality of $j_{44}$. It then follows that

$$\mathrm{tr}(\mathbf{B}) = -(D + \delta Y\mu_{2C}) \;\&\; \det(\mathbf{B}) = \delta Y\mu_2\mu_{2C} \tag{A8}$$

Positivity of $\det(\mathbf{B})$ requires that $\mu_{2C}$ be positive and implies negativity of $\mathrm{tr}(\mathbf{B})$. A coexistence steady state with nonpositive $\mu_{2C}$ is, therefore, unstable. Since $\mu_{2C} \leq 0$ for $C = C_2 \geq C_m$ (Figure 2b) steady states $CO3$ and $CO4$, are obviously unstable (Table 2).

For a coexistence or partial washout steady state, the characteristic equation for **A** assumes the form

$$\lambda^3 + a_1\lambda^2 + a_2\lambda + a_3 = 0 \tag{A9}$$

with

$$a_1 = (2D + \alpha X + \beta\mu_{1B}X), \quad a_2 = (D + \alpha X)(D + \beta\mu_{1B}X) - \mu_{1B}X(\alpha A - \beta\mu_1), \quad a_3 = \mu_{1B}X[\alpha\beta\mu_1 X - D(\alpha A - \beta\mu_1)] \tag{A10}$$

For stability of a coexistence or partial washout steady state, it is necessary that the real parts of the eigenvalues of **A** be negative. The necessary and sufficient conditions for this are obtained by applying the Routh-Hurwitz criteria,[28] leading to the following conditions for local, asymptotic stability

$$a_1 > 0, \qquad a_3 > 0, \qquad b_1 > 0, \qquad b_1 = \left(a_2 - \frac{a_3}{a_1}\right) \tag{A11}$$

Substituting the second relation in Eq. 14 and Eq. 17 into the expression for $a_3$ in Eq. A10 followed by some algebraic manipulation, it can be deduced that

$$a_3 = \frac{\mu_{1B}\sqrt{\Delta}}{2\alpha\beta\mu_1}\rho(X), \qquad \rho(X_1) = (\sqrt{\Delta} - \phi), \quad \rho(X_2) = (\sqrt{\Delta} + \phi) \tag{A12}$$

It is obvious from Eq. 17 that $\rho(X_1) < 0$ and $\rho(X_2) > 0$. Since $\mu_{1B} > 0$ (Eq. 8 and Figure 2a) it follows that $a_3 \leq 0$ for $X = X_1$ [$a_3 = 0$ when $X_1 = X_2$ or $A_0 = \psi(D)$], and the steady states $PW1$, $CO1$, and $CO3$ are unstable (Table 2).

In summary, out of the six steady states involving retention of $X$, only $PW2$ and $CO2$ *may* be stable. For these steady states, one of the conditions for stability, namely $a_1 > 0$, is automatically satisfied since $\mu_{1B} > 0$ (Eq. A10). The necessary and sufficient condition(s) for local, asymptotic stability of these steady states, therefore, are

$$b_1 > 0, \quad A_0 > \psi(D) \; (a_3 > 0), \text{ and (1) for } CO2\text{: } C_1 < C_m(\mu_{2C} > 0), \text{ (2) for } PW2\text{: } \bar{C}_2 < C_1 \text{ or } \bar{C}_2 > C_2 \text{ if } 0 < D \leq (\mu_{2m} - k_2) \tag{A13}$$

If locally stable, a transition in stability characteristics of steady states $PW2$ and $CO2$ may occur upon change in oper-

ating conditions if one or more eigenvalues of **J** (and, hence, **A** and **B**) cross the imaginary axis. If a real eigenvalue of **A** or **B** crosses the imaginary axis while the other four eigenvalues of **J** have negative real parts, there will be a static bifurcation. The loss of stability of a steady state in this case is accompanied by emergence (branching) of other steady states. For this, it is necessary that (1) $a_3 = 0$ (Eq. A9), that is, $X_1 = X_2$ or $A_0 = \psi(D)$ (Eq. A12) or (2) $\det(\mathbf{B}) = 0$ (Eq. A6). The necessary and sufficient conditions for static bifurcation for $CO2$, therefore, are ($\det(\mathbf{B})$ in Eq. A8)

$$A_0 = \psi(D), \qquad b_1 > 0, \qquad C_1 < C_m \tag{A14}$$

or

$$C_1 = C_m\,(\mu_{2C} = 0), \qquad A_0 > \psi(D), \qquad b_1 > 0 \tag{A15}$$

Similarly, based on the preceding discussion, the necessary and sufficient conditions for a static bifurcation for $PW2$ are obtained as

$$A_0 = \psi(D), \qquad b_1 > 0, \text{ and } \bar{C}_2 < C_1 \text{ or } \bar{C}_2 > C_2 \text{ if } 0 < D \leq (\mu_{2m} - k_2) \tag{A16}$$

or

$$\bar{C}_2 = C_1 \text{ or } C_2 \quad \text{if} \quad 0 < D \leq (\mu_{2m} - k_2), \quad A_0 > \psi(D), \qquad b_1 > 0 \tag{A17}$$

The condition $A_0 = \psi(D)$ in Eqs. A14 and A16 corresponds to collision (merger) of steady-state pairs (1) $CO1$ and $CO2$, (2) $CO3$ and $CO4$, and (3) $PW1$ and $PW2$ as $X_1 = X_2$ (Table 2). The condition $C_1 = C_m$ in Eq. A15 corresponds to collision/merger of steady-state pairs (1) $CO1$ and $CO3$, and (2) $CO2$ and $CO4$, as $C_1 = C_2$ (Table 2). It will be seen later that condition $\bar{C}_2 = C_1$ or $C_2$ in Eq. A17 corresponds to birth (emergence) of coexistence steady states $CO2$ ($\bar{C}_2 = C_1$) and $CO4$ ($\bar{C}_2 = C_2$) from $PW2$.

If a pair of complex eigenvalues of **J** crosses the imaginary axis, while the remaining eigenvalues have negative real parts, then there will be a Hopf bifurcation, leading to periodic solutions emanating from the steady states $CO2$ and $PW2$. For this to occur, the characteristic equation for **A** (Eq. A9) or **B** (Eq. A6) must have a pair of imaginary roots. For **B**, this requires that $\mathrm{tr}(\mathbf{B}) = 0$ and $\det(\mathbf{B}) > 0$. The eigenvalues of **B** for $PW2$ are real (Eq. A7). For $CO2$, positivity of $\det(\mathbf{B})$ implies negativity of $\mathrm{tr}(\mathbf{B})$ (Eq. A8). The eigenvalues of **B** cannot, therefore, be imaginary for both $CO2$ and $PW2$. For Hopf bifurcation, the characteristic equation for **A** (Eq. A9) must have a pair of imaginary roots, $\lambda = \pm pi$, implying that $(\lambda^2 + p^2)$ must be a factor in the characteristic equation. Rewriting Eq. A9 as

$$\lambda(\lambda^2 + a_2) + a_1\left(\lambda^2 + \frac{a_3}{a_1}\right) = 0 \tag{A18}$$

one can deduce that imaginary eigenvalues of **A** are admissible only if $p^2 = a_2 = a_3/a_1$ or $b_1 = 0$ (Eq. A11). The necessary and sufficient conditions for a Hopf bifurcation, therefore, are

$$b_1 = 0, \qquad A_0 > \psi(D), \text{ and (1) for } CO2\text{: } C_1 < C_m, \quad \text{(2) for } PW2\text{: } \bar{C}_2 < C_1 \text{ or } \bar{C}_2 > C_2 \text{ if } 0 < D \leq (\mu_{2m} - k_2) \tag{A19}$$

It should be obvious from conditions in Eq. A13 that for $0 < D < (\mu_{2m} - k_2)$ [$C_1 < C_m$], (1) local stability of $PW2$ implies local stability of $CO2$, if physically realizable, and (2) instability of $CO2$, if physically realizable, implies instability of $PW2$.

For very low $D$, it can be deduced that $\phi$, $\sqrt{\Delta}$, and, therefore, $X_2$ are of the order of $D$, $O(D)$ (Eqs. 16 and 17), and, therefore, $a_3$ is $O(D^2)$, $a_1$ is $O(D)$, and $a_3/a_1$ is $O(D)$ (Eq. A10). Furthermore, the first term in the expression for $a_2$ in Eq. A10 is $O(D^2)$, and the second term is $O(D)$. Hence, the negative terms in the expression for $b_1$ in Eq. A11 are $O(D)$, while the positive term is $O(D^2)$, leading to a negative $b_1$ in the vicinity of $D = 0$. In the immediate neighborhood of $D = 0$, therefore, both $PW2$ and $CO2$ are unstable (Eq. A13). Local stability of either steady state for some $D$ then requires occurrence of Hopf bifurcation.

*Manuscript received Jun. 29, 2005, revision received Feb. 24, 2006, and final revision received Apr. 27, 2006.*